CYTOTOXIC EVALUATION AND FACTORIAL ANALYSIS OF 3D PHOTOPOLYMERIZABLE THERMORESPONSIVE COMPOSITE NANOPARTICLE HYDROGELS FOR CONTROLLED DRUG DELIVERY IN RESTENOSIS AND WOUND HEALING

by

ABHIMANYU RAJARAM SABNIS

Presented to the Faculty of the Graduate School of

The University of Texas at Arlington in Partial Fulfillment

of the Requirements

for the Degree of

MASTER OF SCIENCE IN BIOMEDICAL ENGINEERING

THE UNIVERSITY OF TEXAS AT ARLINGTON

AUGUST 2007

ACKNOWLEDGEMENTS

I would like to thank Dr. Kytai Nguyen for giving me the opportunity to work in her laboratory. Under her guidance, I have learnt how to approach a research problem and utilize my critical thinking to develop a simple feasible solution. Her faith in my ability gave me the opportunity to pursue this project independently and develop my analytical skills. Dr. Nguyen has always been a source of inspiration and a pillar of support throughout the duration of my graduate studies.

I would also like to thank Dr. Pranesh Aswath and Dr. Jian Yang for agreeing to serve on my thesis committee. I would also like to thank all my lab mates in the Nanomedicine and Tissue Engineering Lab. In particular, I would like to thank Maham Rahimi, Chris Chapman, Hao Xu and Priya Nattama. A special thanks to Aniket Wadajkar who has been with me through the highs and lows of this project.

Last but not the least; I would like to thank my family for their love and support throughout my life. Without their best wishes, I would not have been able to fulfill my dreams.

July 17, 2007

ABSTRACT

CYTOTOXIC EVALUATION AND FACTORIAL ANALYSIS OF 3D PHOTOPOLYMERIZABLE THERMORESPONSIVE COMPOSITE NANOPARTICLE HYDROGELS FOR CONTROLLED DRUG DELIVERY IN RESTENOSIS AND WOUND HEALING

Publication No. _____

Abhimanyu Rajaram Sabnis, M.S.

The University of Texas at Arlington, 2007

Supervising Professor: Dr. Kytai T. Nguyen

To develop a smart drug delivery system for restenosis and wound healing applications, we investigated photopolymerizable composite nanoparticle hydrogels which can release the drug in a temperature-responsive manner. Our novel system consisting of thermoresponsive poly(*N*-isopropylacrylamide-co-acrylamide) (PNIPA-AAm) nanoparticles and poly(ethylene glycol) diacrylate (PEGDA) as photo cross-linker can be formed *in situ* in presence of ultraviolet (UV) light and Irgacure 2959

photoinitiator (PI). The main aims of this project were to investigate the system cytotoxicity and optimize drug release characteristics by performing biocompatibility and factorial analysis studies, respectively. We evaluated the cell survival of human vascular smooth muscle cells and NIH/3T3 fibroblasts upon exposure to UV light and photoinitiator concentrations. At conditions required for photopolymerization of our composite system (UV=5 minutes, PI=0.015% w/v), the cell survival for both cell types was not significantly decreased. Addition of an anti-oxidant reagent, ascorbic acid, to hydrogel precursor solution further improved cell survival at higher PI concentrations, but increased the gelation times. Additionally, we performed a factorial analysis to evaluate the effects of PEGDA concentration (10% and 15% w/v) and molecular weight (3.4 KDa and 8 KDa) as well as PNIPA-AAm nanoparticle concentration (2% and 4% w/v) on the hydrogel gelation times, drug release profiles and swelling ratios. Our studies showed PNIPA-AAm nanoparticle concentration was the most important factor affecting the drug release at 40^{o}C and thermoresponsiveness of the system. Additionally, PEGDA concentration affected gelation times while PEGDA molecular weight governed the swelling ratio. These findings have improved our understanding of the composite systems and will help in tailoring future systems with desired characteristics.

TABLE OF CONTENTS

ACKNOWLEDGEMENTS ii

ABSTRACT iii

LIST OF ILLUSTRATIONS viii

LIST OF TABLES xi

Chapter

1. INTRODUCTION…….. 1

1.1 Restenosis …… 1

1.1.1 Coronary Artery Disease and Modes of Treatment 1

1.1.2 Current Methods for Prevention of Restenosis and Their Associated Problems 2

1.2 Wound Healing……. 3

1.2.1 Biological Mechanisms of Normal Wound Healing 3

1.2.2 Moist Wound Healing 4

1.2.3 Types of Occlusive Dressings and Their Associated Problems…. 4

1.3 Our Novel Photopolymerizable Thermoresponsive Composite Nanoparticle Hydrogels…….. 5

1.3.1 Overview of Our System 5

1.3.2 Advantages of Our Composite Nanoparticle Hydrogels 10

1.3.3 Specific Aims 10

1.3.4 Successful Outcome of This Research Project 11

2. CYTOTOXIC EVALUATION OF THE COMPOSITE HYDROGELS… . 12

2.1 Introduction……..... 12

2.2 Materials and Methods 13

2.2.1 Materials……... 13

2.2.2 Human Aortic Smooth Muscle Cell (HASMC) and NIH/3T3 Fibroblast Cell Culture..... 13

2.2.3 Effects of UV Exposure Durations 14

2.2.4 Effects of Photoinitiator Concentrations 14

2.2.5 Combined Effects of Photoinitiator and UV Exposure 15

2.2.6 Preparation of PNIPA-AAm Nanoparticles..... 15

2.2.7 Preparation of Photopolymerized Thermoresponsive Hydrogels 16

2.2.8 Effect of Antioxidants..... 16

2.2.9 Cell Survival Using Pico-Green DNA Assays 17

2.2.10 Statistical Analysis..... 17

2.3 Results……..... 18

2.3.1 Effects of UV Exposure Durations 18

2.3.2 Effects of Photoinitiator Concentrations 19

2.3.3 Combined Effects of Photoinitiator and UV Exposure 21

2.3.4 Effect of Antioxidants..... 24

2.4 Discussion……..... 25

2.5 Conclusion……. 29

3. FACTORIAL ANALYSIS..... 30

3.1 Introduction……..... 30

3.2 Materials and Methods……..... 31

3.2.1 Preparation of poly(ethylene glycol) (PEGDA) 31

3.2.2 Factorial Analysis using Design of Experiments 32

3.2.3 Preparation of Photopolymerized Thermoresponsive Hydrogels 34

3.2.4 Effects on Gelation Time..... 34

3.2.5 Effects on Drug Release 35

3.2.6 Effects on Swelling Ratio 35

3.3 Results……..... 36

3.3.1 Effects on Gelation Time 36

3.3.2 Effects on Drug Release..... 39

3.3.2.1 Dependence of Drug Release on Factors..... 41

3.3.2.2 Dependence of Thermoresponsiveness on Factors.... 54

3.3.3 Effects on Swelling Ratio..... 58

3.4 Discussion…….. 61

3.5 Conclusion…….. 65

4. CONCLUSION…… 67

5. LIMITATIONS AND FUTURE WORK 69

REFERENCES 71

BIOGRAPHICAL INFORMATION..... 79

LIST OF ILLUSTRATIONS

Figure Page

1.1 Principle of the photopolymerizable thermoresponsive composite nanoparticle hydrogels. 6

1.2 (a) Comparison of identical composite nanoparticle hydrogels incubated at 25^{o}C (left) and 40^{o}C (right). (b) SEM image of composite nanoparticle hydrogels nanoparticles with 20% (w/v) PNIPA-AAm nanoparticles..... 9

2.1 The effects of varying durations of long wave, 365 nm UV light exposure at about 10 mW/cm^2 on the survival of human aortic smooth muscle cells and NIH/3T3 fibroblasts. 19

2.2 The effects of photoinitiator (Irgacure 2959) concentrations on the survival of human aortic smooth muscle cells and NIH/3T3 fibroblasts in absence of UV light..... 21

2.3 The combined effects of photoinitiator concentrations and UV exposure on the cell survival. (a) Human aortic smooth muscle cells. (b) NIH/3T3 fibroblasts..... 23

2.4 Effect of Ascorbic Acid on the HASMC cell survival when exposed to 0.15% (w/v) Irgacure 2959 and 5 minutes of UV exposure..... 24

3.1 The effects of the 3 factors on gelation time. 37

3.2 Variation in gelation time with (a) 10% (w/v) and (b) 15% (w/v) PEGDA concentration. 38

3.3 Cumulative drug release profiles of the different composite systems as an effect of the 3 factors..... 39

3.4 Drug release profiles at 25^{o}C and 40^{o}C……..... 40

3.5 Drug release rates for different hydrogels (Run 1-4) at both 25°C and 40°C. 42

3.6 Effect of factors on drug release rates at 25°C……. 43

3.7 Variation in drug release rate at 25°C with (a) 10% (w/v) and (b) 15% (w/v) PEGDA concentration. 44

3.8 Effect of factors on drug release rates at 40°C. 45

3.9 Variation in drug release rate at 40°C with (a) 2% (w/v) and (b) 4% (w/v) PNIPA-AAm nanoparticle concentration. 46

3.10 Drug release rates at 40°C for t_1 = 0 hrs and t_2 = 8 hrs. 48

3.11 Effect of factors on the drug release rates at 40°C for t_1 = 0 hrs and t_2 = 8 hrs……..... 49

3.12 Variation in drug release rate at 40°C with (a) 2% (w/v) and (b) 4% (w/v) PNIPA-AAm nanoparticle concentration. (t_1 = 0 hrs and t_2 = 8 hrs)…….....50

3.13 Drug release rates at 40°C for t_1 = 8 hrs and t_2 = 48 hrs…….. 51

3.14 Effect of factors on the drug release rates at 40°C for t_1 = 8 hrs and t_2 = 48 hrs……..… 52

3.15 Variation in drug release rate at 40°C with (a) 3.4 kDa and (b) 8 kDa MW PEGDA. (t_1 = 8 hrs and t_2 = 48 hrs)…… 53

3.16 Difference between the drug release rates at 25°C and 40°C for the 4 hydrogel runs (up to 8 hrs)…….. 55

3.17 Effect of the factors on the thermoresponsiveness of the 4 hydrogel runs (up to 8 hrs)…….. 56

3.18 Variation in difference between drug release rates at 25°C and 40°C with (a) 2% (w/v) and (b) 4% (w/v) PNIPA-AAm nanoparticle concentration. (t_1 = 0 hrs and t_2 = 8 hrs)…….. 57

3.19 Effect of the factors on the hydrogel swelling ratio……. 59

3.20 Variation in swelling ratio with (a) 3.4 kDa MW PEGDA and (b) 8 kDa MW PEGDA……..... 60

LIST OF TABLES

Table Page

3.1 Low and High Levels for the Half Factorial Design 33

3.2 Coded Values of the Half Factorial Design 33

3.3 Actual Values of the Half Factorial Design 33

3.4 Effects of Factors on Gelation Time 36

3.5 Drug Release Rates at t_1 = 0 hours and t_2 = 48 hours 41

3.6 Drug Release Rates at 40^{o}C 47

3.7 Effects of Factors on Swelling Ratio 58

CHAPTER 1

INTRODUCTION

1.1 Restenosis

1.1.1. Coronary Artery Disease and Modes of Treatment

Coronary arteries are responsible for supplying oxygen-rich blood to the heart. When plaque builds up in these arteries, blood flow to the heart will be reduced. This leads to the heart being deprived of oxygen, causing symptoms ranging from mild chest pain to a fatal heart attack.[1] This plaque buildup process is called atherosclerosis and is usually treated either by coronary artery bypass surgery (CABG) or by percutaneous transluminal angioplasty (PTCA), depending on the degree of plaque buildup.[1] CABG is a process by which the diseased portion of the artery is bypassed by grafting a conduit taken from the healthy saphenous vein. CABG is often used to treat arteries with a high degree of plaque buildup. This procedure is highly invasive and involves opening the chest cavity, sawing the sternum and performing cardiopulmonary bypass. CABG can be traumatic to patients and causes damage to the blood being passed through the heart-lung machine when patient undergoes surgical procedure. In addition, chest infection could require a second cardiac surgery, thereby increasing trauma to the patients.

PTCA is a much less invasive procedure and is the most common mode of treatment to treat coronary artery disease with lesser plaque buildup. An estimated 850,000 PTCA procedures are carried out annually compared with 390,000 CABG

surgeries.[2] This procedure involves entry of the catheter through a major artery, and concurrent progress of the catheter to the aorta under fluoroscopic guidance. The catheter is then led to the left or right coronary artery, and positioned precisely at the obstruction. The balloon located at the tip of the catheter is inflated one or more times so that the plaque is pressed up against the arterial wall, thereby clearing the obstruction. Once the balloon is deflated, the catheter is retrieved and the wound is closed. However, PTCA involves the risk of re-narrowing of the treated artery within six months of surgery. Restenosis, the re-narrowing of the treated artery, is caused by a major loss of the endothelial cell population (a natural vascular barrier), the adherence and deposition of blood cells as well as resultant smooth muscle cell (SMC) migration, and subsequent proliferation at the injured arterial wall site.[3-5] Restenosis needs to be treated immediately, usually by a repeat PTCA procedure.

1.1.2. Current Methods for Prevention of Restenosis and Their Associated Problems

To reduce restenosis after PTCA, several strategies such as implanting bare metal stents and drug eluting stents have been used. For a stenting procedure, a metallic stent is implanted following inflation of balloon in PTCA. Results from stenting have shown a reduction in the occurrence rates of restenosis. However, 20-30% of patients undergoing coronary intervention with stent implantation require repeat procedures.[6] PTCA causes enlargement (and weakening) of the lumen and damage of the endothelial monolayer lining the blood vessel. This leads to the exposure of the medial layer to the

circulating blood, and thus results in platelet activation and aggregation, with the potential for formation of a platelet-rich thrombus and acute restenosis.

Recently, drug eluting stents have been developed to reduce the chances of restenosis. Drug eluting stents can be of two types, namely stents which are coated with drugs, and stents which have a polymeric coating loaded with the drug. Polymer loaded stents incorporating sirolimus and paclitaxel are already in the market. These stents have been able to drastically reduce the chances of restenosis by delivering the drug over an extended period of time. However, the problem associated with stents, remains to be that of biocompatibility and thrombogenicity. Drug coated stents are also unable to release the drug over a longer time, thereby only delaying the occurrence of restenosis. Significant research has shown that patients implanted with drug eluting stents (DES) show a larger risk of late stent thrombosis (>30 days) as compared to bare metal stents (BMS). This risk is significant as fatal occlusions and myocardial infarctions are noted in a large percentage of those patients that exhibit late stent thrombosis (LAST).[7-9]

1.2 Wound Healing

1.2.1. Biological Mechanisms of Normal Wound Healing

The general mechanism for normal healing of wounds follows three overlapping phases.[10,11] The first event involves activation of the coagulation cascade, formation of a blood clot followed by inflammation. The second stage consists of granulation tissue formation where a weak tissue is formed to temporarily act as the lost tissue. Matrix

remodeling, formation of new blood vessels and replacement of the lost tissue by strong identical tissue occurs in the final stage of wound healing.[10,11]

1.2.2. Moist Wound Healing

Moist wound healing involves the healing of wounds under moist conditions. As described by Turner, an ideal wound dressing should be able to maintain high humidity at the wound-dressing interface.[12] Such wound dressings which are able to keep the wounded area moist and thus promote moist wound healing are called occlusive dressings.[13] The advantages of using moist wound healing over air drying of wounds include reduced dehydration and cell death, improved angiogenesis, increased re-epithelialization, formation of bacterial barrier and reduced infection rates, and decreased patient discomfort.[14] In addition, although occlusive dressings have a higher initial cost, they require fewer dressings and reduce recovery time, therefore resulting in reduced overall costs.[14]

1.2.3. Types of Occlusive Dressings and Their Associated Problems

It is estimated that there are around 1000 different types of occlusive dressings available and these include films, foams, hydrocolloids and hydrogels.[13] The choice of occlusive dressing depends upon the wound type and also surrounding area. For example, hydrogels are effective for highly exudating wounds.[13] Films are usually polyurethane based, retain moisture and are transparent, thereby allowing visual observation of the wound without removal of dressing. However, films exhibit limited

or no absorption of the wound fluids.[13] Foams are also polyurethane based, absorb large amounts of wound fluids and are best suited for wounds with heavy exudate. Foams, however, can dry the wound in absence of sufficient exudate.[13] Hydrocolloids are best suited for wounds that exudate up to moderate volumes of wound fluid as heavy exudation cannot be handled by this type of wound dressing. In addition, these dressings can break down in the wound and residue removal requires a lot of time.[13] Hydrogels are water based dressings which maintain a moist (not wet) micro environment at the wound. These dressings are simple to apply and remove, allow greater comfort and provide a moist environment which promotes the cell migration.

1.3 Our Novel Photopolymerizable Thermoresponsive Composite Nanoparticle Hydrogels

1.3.1. Overview of Our System

Our long term goal is to develop *in situ* photopolymerizable thermoresponsive composite nanoparticle hydrogels to aid in preventing restenosis and improving wound healing. Our system, consisting of poly(*N*-isopropylacrylamide-co-acrylamide) (PNIPA-AAm) thermoresponsive nanoparticles, photo cross-linker poly(ethylene glycol) diacrylate (PEGDA) and UV photoinitiator 2-hydroxy-1-[4-(2-hydroxyethoxy) phenyl]-2-methyl-1-propanone (Irgacure 2959), would be photopolymerized at the injury site for local drug delivery. The principle of our system, as shown in Figure 1.1, can be briefly described as follows. Following injury or angioplasty, a precursor solution comprised of the drug-loaded PNIPA-AAm nanoparticles, photoinitiator, and PEGDA photo cross-linker solution would be delivered to the injury site. In the

presence of UV light, these materials would form a hydrogel network entrapping the PNIPA-AAm nanoparticles, coating the injured area, and forming a protective barrier. Upon reaching body temperature, the PNIPA-AAm nanoparticles would undergo a reversible phase transition, collapse, and expel the drugs into the surrounding environment.

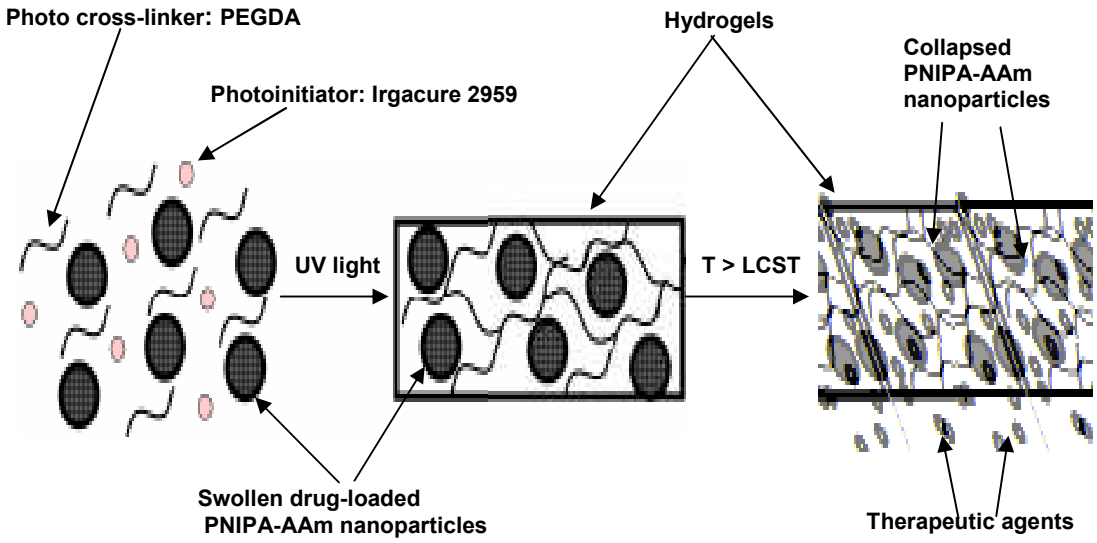

Figure 1.1 Principle of the photopolymerizable thermoresponsive composite nanoparticle hydrogels.

Photopolymerization of hydrogels has been investigated extensively for use in various biomedical applications, including drug delivery [15-19] and tissue engineering.[20-28] Upon exposure to UV light, photopolymerization allows rapid conversion of a liquid monomer or macromer solution into a gel *in situ*.[29,30] Other advantages of photopolymerized hydrogels include spatial and temporal control of reaction kinetics,

fast curing rates to provide rapid polymerization, and effective control over cross-linking density thereby governing the release rate.[31-33] These advantages make photopolymerized hydrogels extremely desirable as systems for smart local drug delivery and cell microencapsulation.[30]

The essential components needed to form a photopolymerized hydrogel network are the photo cross-linker, photoinitiator and UV irradiation. Poly(ethylene glycol) (PEG) functionalized with diacrylate group (PEGDA) was chosen as the photo cross-linker, as it cross-links quickly in the presence of UV light and photoinitiator to form hydrogels.[30,34] Additionally, PEGDA is considered biocompatible and nontoxic as it is a derivative of PEG.[35] When photoinitiator molecules are exposed to specific wavelengths of visible or UV light, they dissociate into free radicals, which initiates the polymerization reaction.[29,30]

The inclusion of poly(*N*-isopropylacrylamide) (PNIPA) based nanoparticles enables this system to release the drug in a thermoresponsive manner. At its lower critical solution temperature (LCST, around 32^{o}C), PNIPA undergoes a reversible phase transition in aqueous solutions. At temperatures below the LCST, PNIPA exhibits hydrophilic properties and exists in an individual chain with a coil conformation. Above the LCST, hydrophobic attractions become more favorable, resulting from a sharp transition from the coil to globule conformation.[34] This unique property of PNIPA, to undergo a reversible phase transition at temperatures close to body temperature, makes it desirable for biomedical applications,[6,36-39] including drug delivery.[40-42]

The LCST of PNIPA can be further increased to normal body temperature by copolymerizing with hydrophilic monomers, such as PEG.[34,43] Previous work in our lab, by Rahimi and Wadajkar, had increased LCST to 40°C by copolymerizing *N*-isopropylacrylamide with acrylamide. Rahimi and Wadajkar also showed that this PNIPA – Acrylamide (PNIPA-AAm) copolymer has a sharper phase transition compared to PNIPA alone. Since PNIPA-AAm is closer to the body temperature range, we incorporated PNIPA-AAm nanoparticles into our system instead of PNIPA. Utilizing the thermoresponsive property of the PNIPA-AAm copolymer allows us to load the hydrophilic drug at a low temperature and release it *in vivo* upon equilibration of PNIPA-AAm to normal body temperature. Delivery of bioactive molecules such as proteins, genes, and peptides would be potential benefits of our composite hydrogel system compared to other drug delivery carriers as these molecules are easily denatured by heat and organic solvents.

A comparison of two identical composite hydrogel systems maintained at two different temperatures, i.e. 25°C and 40°C, as well as a SEM image of the composite system is shown in Figure 1.2.

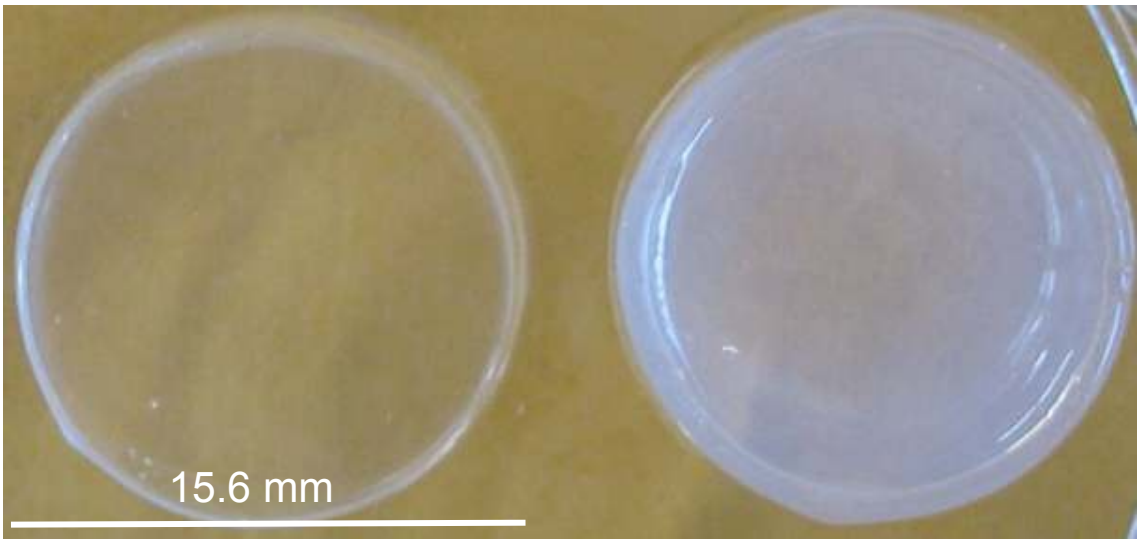

(a)

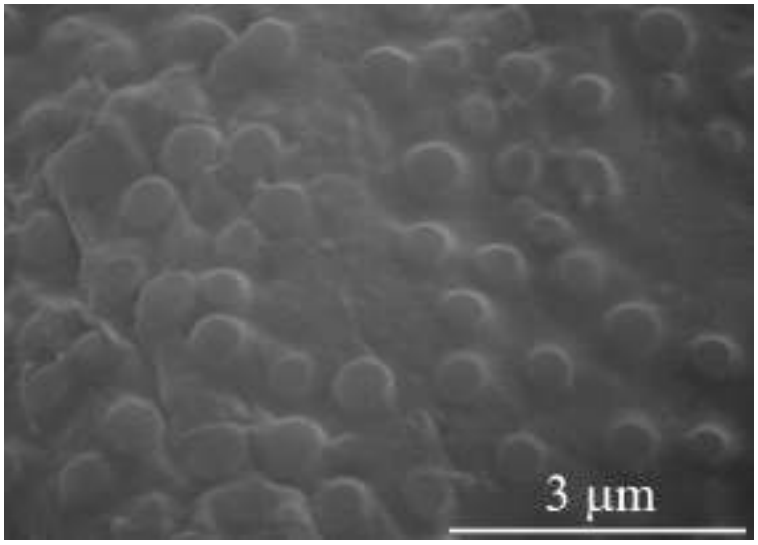

(b)

Figure 1.2 (a) Comparison of identical composite nanoparticle hydrogels incubated at 25^{o}C (left) and 40^{o}C (right). (b) SEM image of composite nanoparticle hydrogels with 20% (w/v) PNIPA-AAm nanoparticles.

1.3.2. Advantages of Our Composite Nanoparticle Hydrogels

The advantage of our composite nanoparticle hydrogels that it would provide both local and stimuli-responsive drug delivery capable of releasing a drug in response to temperature changes.[34] The LCST of PNIPA-AAm nanoparticles (40^{o}C) can be used for applications like wound healing, where heat is applied externally in an on-off fashion to accurately control the release of drug. In addition to releasing the drug in a temperature responsive manner, the hydrogel film would also act as a protective barrier against the recruitment of blood cells such as platelets and leukocytes, major causes of thrombosis and inflammation at the damaged arterial wall.[44] Another advantage of our system would be its ability to photopolymerize directly at the injury site. Once developed, these composite hydrogels would provide the physician easy implantation and effective control over the release of the drug by applying heat to the composite system thus administering drug only when required.

1.3.3. Specific Aims

To develop the 3D photopolymerizable thermoresponsive composite hydrogel nanoparticle system, two specific aims were pursued.

- Aim 1: Evaluate the cytotoxicity of composite system components such as UV exposure, photoinitiator concentrations and free radicals released during photopolymerization.
- Aim 2: Perform factorial analysis to determine the effect of factors such as PEGDA molecular weight, PEGDA concentration and PNIPA-AAm nanoparticle

concentration on the composite hydrogel's gelation time, drug release profile, thermoresponsiveness, and swelling ratio.

1.3.4. Successful Outcome of This Research Project

The successful outcome of this project would provide an improved understanding of the cytotoxicity of the composite system and the factorial influence on system characteristics. It is expected that this study will help in designing composite systems with specific drug release and thermoresponsive profiles while maintaining biocompatibility of the system.

CHAPTER 2

CYTOTOXIC EVALUATION OF THE COMPOSITE SYSTEM

2.1 Introduction

The use of UV light and photoinitiator molecules makes it necessary to determine the compatibility of these composite nanoparticle hydrogels for biomedical applications. The UV photoinitiator Irgacure 2959 was selected based on the results of previous studies that Irgacure 2959 was the most cytocompatible UV photoinitiator compared to other photoinitiators for different cell types.[29,31,45] However, one such study on the effect of Irgacure 2959 also noted that different cell types displayed different sensitivities to the same concentration of this photoinitiator.[31] Therefore, it is essential to determine the sensitivity of HASMCs and NIH/3T3 fibroblast cells specifically to Irgacure 2959. Additionally, the cells can undergo cellular damage during photopolymerization as a result of exposure to photoinitiator molecules, reactive macromers, and free radicals.[29]

For our system, inhibiting HASMC migration and proliferation is necessary to prevent restenosis. However, the photoinitiating system must not have a deleterious effect on the existing HASMC population. Similarly, for wound healing applications, further damage to fibroblasts by the system cytotoxicity cannot be tolerated. To prevent damage to the cells present, it is critical to evaluate and minimize the cytotoxicity of the system components. Thus, the aim of this research work was to evaluate the cytotoxic

effects of the composite system components, mainly the photoinitiator and UV light, on the HASMCs and NIH/3T3 fibroblast cells. These cells were exposed to different photoinitiator concentrations and/or UV light exposure for various periods. Cell survival after the exposure was then determined by PicoGreen DNA assays. Ascorbic acid, an antioxidant, was also tested for its efficiency in reducing the cytotoxicity of free radicals. Finally, studies were performed to evaluate the effect of antioxidant addition on the gelation time of our composite hydrogels.

2.2 Materials and Methods

2.2.1. Materials

Chemicals, if not specified, were purchased from Sigma-Aldrich (St. Louis, MO), including *N*-isopropylacrylamide (NIPA), *N, N'*-methylenebisacrylamide (BIS), potassium persulfate (KPS), and sodium dodecyl sulfate (SDS).

2.2.2. Human Aortic Smooth Muscle Cell (HASMC) and NIH/3T3 Fibroblast Culture

Human aortic smooth muscle cells (Cascade Biologics, Portland, OR) and NIH/3T3 fibroblast cells were cultured in complete medium consisting of Dulbecco's Modified Eagle Medium (DMEM) supplemented with 10% fetal bovine serum (FBS) and 1% penicillin-streptomycin (Invitrogen, Carlsbad, CA). Experiments were performed separately on both cell types to evaluate the cytotoxic effects of the composite system. Upon 80-90% confluency, the cells were passaged or used for experiments. For all experiments, the cells were seeded in 24-well plates (Corning Inc., Corning, NY) at a density of 7000 cells/well. Following seeding, the cells were

incubated at 37°C and 5% CO_2 in a humid environment for 2 days to allow cellular attachment and growth. After 2 days, the HASMCs and fibroblasts were exposed to varying concentrations of the photoinitiator Irgacure 2959 (Ciba Specialty Chemicals, Tarrytown, NY) and/or UV exposure.

2.2.3. Effects of UV Exposure Durations

To evaluate the effects of UV exposure on cell survival, HASMCs and fibroblasts were seeded and cultured as described above. The cells were then exposed to varying durations (1, 3, and 5 minutes) of long wave, 365 nm UV light (Model B-100AP/R, UVP) at about 10 mW/cm^2. These durations of UV exposure were chosen because they are sufficient to photopolymerize the hydrogels. Cells not exposed to UV light served as the control. Following exposure, the cells were incubated for another 3 days before lysing to evaluate the cell survival.

2.2.4. Effects of Photoinitiator Concentrations

To evaluate the cytotoxic effects of photoinitiator concentrations on HASMCs and fibroblasts, the cells were seeded and cultured as described above. Irgacure 2959 was directly dissolved in complete media to obtain final concentrations of 0.01%, 0.02%, 0.04%, 0.08%, and 0.16% (w/v). These photoinitiator concentrations were well within the range required for photopolymerization in a short period of time. The photoinitiator solutions were carefully protected from exposure to light to preserve their activity. These solutions were then sterilized using 0.2 μm syringe filters before adding

to the cells. The control wells consisted of cells incubated with photoinitiator-free complete media. After the addition of the photoinitiator, the cells were incubated for 3 days and then lysed to assess the cell survival.

2.2.5. Combined Effects of Photoinitiator and UV Exposure

The cellular damage due to the combined effects of photoinitiator and UV exposure was evaluated using the previously described method.[31] Briefly, the HASMCs and fibroblasts were seeded onto 24-well plates and allowed to grow for 2 days. Irgacure 2959 solutions with final concentrations of 0.01%, 0.015%, 0.04%, and 0.08% (w/v) in complete media were prepared. After adding these solutions, cells were incubated for 30 minutes to allow for the mixing of the photoinitiator. The well plates were then exposed to 1, 3, and 5 minutes of UV light. Wells containing cells not exposed to either UV light or photoinitiator solution served as controls for this experiment. Cell samples were incubated for 3 days and then lysed to measure the cell survival.

2.2.6. Preparation of PNIPA-AAm Nanoparticles

PNIPA-AAm nanoparticles (100 nm) were prepared by modifying the previously described method.[34,46,47] Briefly, an aqueous solution (100 ml) containing *N*-isopropylacrylamide (1.3644 g), acrylamide (0.1756 g), *N, N'*-methylenebisacrylamide (0.0262 g), and sodium dodecyl sulfate (0.0439 g) was stirred under argon gas for 30 minutes. Potassium persulfate (0.0624 g) was added and emulsion polymerization was

carried out in an oil bath at 70°C for 4 hours under argon. The resulting particles were cooled to room temperature and dialyzed (10 kDa MW cutoff) against deionized water for 4 days to remove unreacted monomer and surfactant.

2.2.7. Preparation of Photopolymerized Thermoresponsive Hydrogels

Photopolymerized hydrogels were produced using the method outlined by Ramanan *et al.*[34] Briefly, PNIPA-AAm nanoparticles (2% w/v) were added to a solution containing PEGDA (MW 3400, NEKTAR Therapeutics, Huntsville, AL) with a final PEGDA concentration of 100 mg/ml. The UV photoinitiator, Irgacure 2959 was then added at a final concentration of 0.015% (w/v). 200 µl of this solution was added to a 48-well plate and exposed to long-wave, 365 nm UV light at about 10 mW/cm^2 for five minutes to form the composite hydrogels.

2.2.8. Effect of Antioxidants

An additional study was performed to evaluate the efficiency of the antioxidant, ascorbic acid, in scavenging the free radicals in an effort to increase cell survival. Ascorbic acid was chosen based on the observation by Williams *et al.* that ascorbic acid present in bovine chondrocyte specific media may be responsible for reducing the cytotoxic effects of Irgacure 2959.[31] HASMCs were exposed to 0.15% (w/v) solution of Irgacure 2959 in complete media supplemented with varying concentrations of ascorbic acid (50-1000mg/L). After incubating for 30 minutes, the cells were exposed to 5 minutes of UV light and lysed after 3 days of incubation.

To evaluate the effect of added antioxidants, the gelation times, i.e. time required for the materials to form a gel, were determined. For this study, 50 mg/L of ascorbic acid was added to the hydrogel precursor solution, containing 0.15% (w/v) Irgacure 2959. The gelation times for hydrogels with or without added ascorbic acid were then compared.

2.2.9. Cell Survival Using Pico-Green DNA Assays

After experiments, cells were lysed with 1 ml of 1% Triton X-100 by incubation for one hour. The lysed samples were analyzed for total cell DNA, which is correlated to the cell number, using PicoGreen DNA assays (Invitrogen) following the manufacturer's instructions. The standard curve was obtained by serial dilution of stock DNA solutions in 1% Triton X-100 and used to calculate the DNA concentrations contained within cell lysate samples. Relative cell survival was obtained by dividing the DNA concentration of a cell sample by the mean DNA concentration of the control.

2.2.10. Statistical Analysis

Analysis of the results was performed using ANOVA tests with $p < 0.05$ (ANOVA StatView 5.0 software, SAS Institute). For each study, four samples were tested ($n = 4$) and all the results are given as mean ± SD.

2.3 Results

2.3.1. *Effect of UV Exposure Durations*

In our study, cells were exposed to UV light in the absence of photoinitiator molecules to determine the effects of UV exposure time only. The HASMCs and fibroblasts were exposed to 1, 3, and 5 minutes of long-wave, 365 nm UV light at about 10 mW/cm^2, which is enough to photopolymerize the hydrogels. Following exposure, cells were cultured for 3 days to evaluate the cytotoxic effects of the UV light. Cells not exposed to ultraviolet light served as the control and were used to determine the relative cell survival rate. The effects of varying durations of UV exposure on the HASMC and fibroblast survival are shown in Figure 2.1. Exposure of HASMCs to 1, 3, and 5 minutes did not show any statistically significant decrease in cell survival and the relative cell survival rates were 1.39 ± 0.32, 1.21 ± 0.07, and 1.20 ± 0.18, respectively. Similarly, UV exposure of NIH/3T3 fibroblast cells for up to 5 minutes did not significantly decrease the cell survival. The relative cell survival rates for the fibroblasts were 1.15 ± 0.049, 0.90 ± 0.05, and 0.95 ± 0.0724 for 1, 3 and 5 minutes of UV exposure respectively.

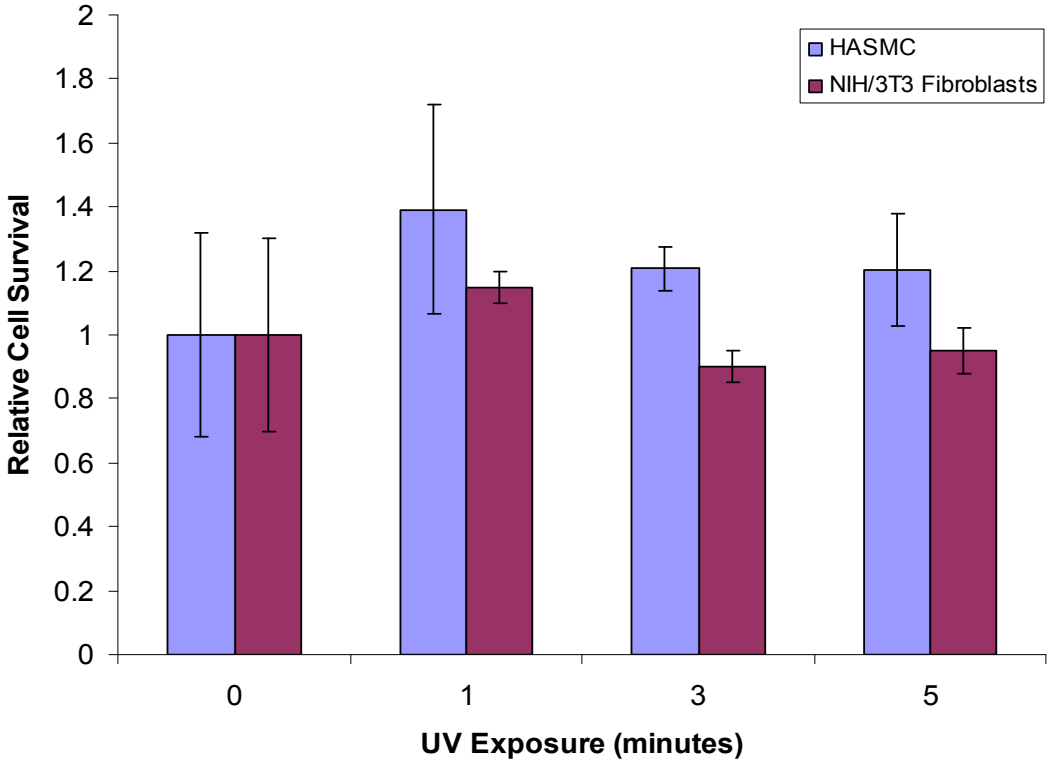

Figure 2.1 The effects of varying durations of long wave, 365 nm UV light exposure at about 10 mW/cm^2 on the survival of human aortic smooth muscle cells and NIH/3T3 fibroblasts. Controls were cells not exposed to UV light (0 minutes of exposure).

2.3.2. *Effect of Photoinitiator Concentrations*

HASMCs and fibroblasts were incubated with various photoinitiator concentrations (0.01%, 0.02%, 0.04%, 0.08%, and 0.016% (w/v) Irgacure 2959) to evaluate the cytotoxicity of photoinitiator molecules. The controls, consisting of wells exposed to photoinitiator-free media, were used to determine relative cell survival. The cytotoxic effects of the varying photoinitiator solutions on HASMCs and fibroblasts are shown in Figure 2.2. Irgacure 2959 did not show a significant decrease in cell survival when HASMCs were exposed to 0.01% (w/v) photoinitiator solution, and relative cell

survival was determined to be 0.981 ± 0.05 (Figure 2.3). However, upon increasing the photoinitiator concentrations above 0.02% (w/v), a statistically significant decrease was noticed in the relative cell survival. Varying the photoinitiator concentration from 0.02% (w/v) to 0.16% (w/v) was found to progressively decrease the relative cell survival from 0.826 ± 0.02 to 0.45 ± 0.04, respectively. NIH/3T3 fibroblast cell survival did not decrease significantly even when exposed to 0.08% (w/v) of Irgacure 2959, and relative cell survival was found to be 0.81 ± 0.13. However, cell survival drastically decreased upon increasing the Irgacure 2959 concentration to 0.16% (w/v), with relative cell survival being 0.37 ± 0.02.

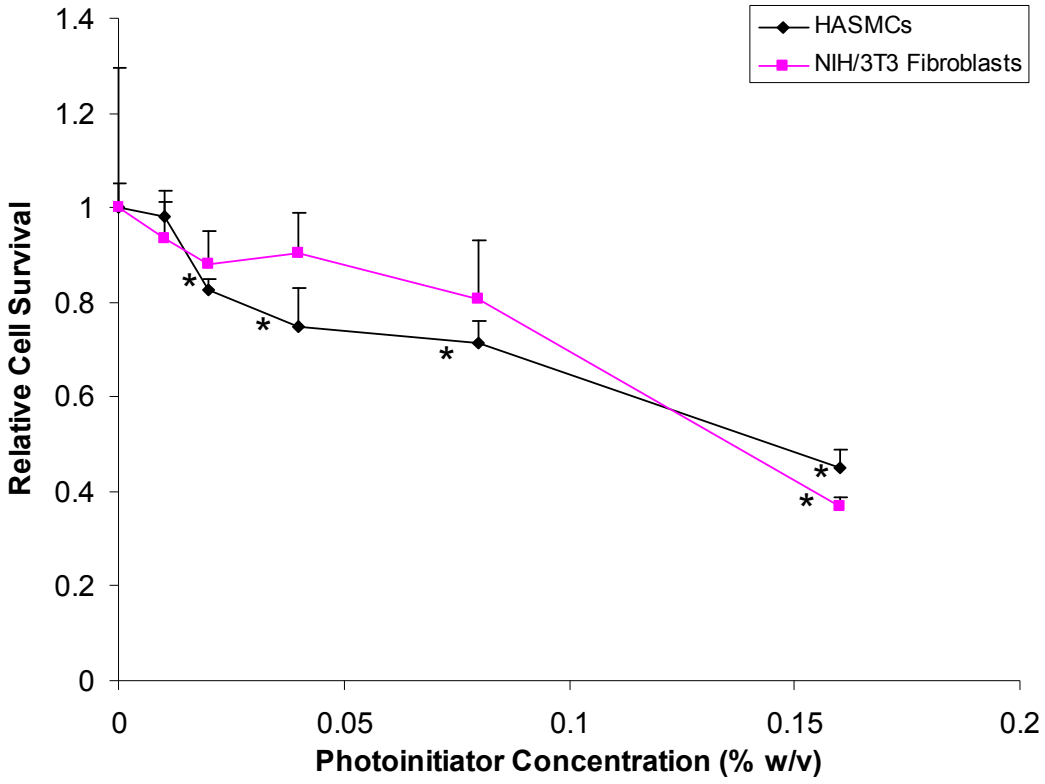

Figure 2.2 The effects of photoinitiator (Irgacure 2959) concentrations on the survival of human aortic smooth muscle cells and NIH/3T3 fibroblasts in absence of UV light. * = Significant Difference ($p<0.05$)

2.3.3. *Combined Effects of Photoinitiator and UV Exposure*

It is essential to evaluate cytotoxic effects of the free radicals formed when photoinitiator molecules are exposed to UV light. For this study, the HASMCs and fibroblasts were treated with photoinitiator solutions (0.01%, 0.015%, 0.04%, and 0.08% w/v) followed by exposure to UV light (1, 3, and 5 minutes). Relative HASMC cell survival, shown in Figure 2.3 (a), was calculated using the control wells which were not exposed to either photoinitiator solution or UV light. For 0.01% and 0.015% (w/v) of photoinitiator concentrations, the HASMCs did not show any statistically significant

decrease in relative cell survival for 1, 3, and 5 minutes exposure (n = 4). At 0.04% (w/v) concentration of Irgacure 2959 in complete media, a significant decrease was observed at 1, 3, and 5 minutes of UV exposure, with relative cell survival values at 0.80 ± 0.016, 0.48 ± 0.07, and 0.55 ± 0.04 of the control samples, respectively. Finally, the relative cell survival rates were significantly reduced at 0.08% (w/v) photoinitiator concentration, ranging between 0.75 ± 0.04 and 0.41 ± 0.07 for the three durations of UV exposure.

For the NIH/3T3 fibroblasts, the cell survival was considerably better than that of HASMCs (Figure 2.3 b). Fibroblast cell survival did not show a significant decrease at any photoinitiator concentration for 1 and 3 minutes of UV exposure, with relative cell survival ranging from 1.18 ± 0.09 to 0.85 ± 0.10. In addition, cell survival was not significantly reduced for 5 minutes of UV exposure and up to 0.04% (w/v) of Irgacure 2959, with a relative cell survival of 0.85 ± 0.07. However, upon exposure of fibroblasts to 0.08% (w/v) and 5 minutes of UV light, relative cell survival decreased to 0.66 ±0.06.

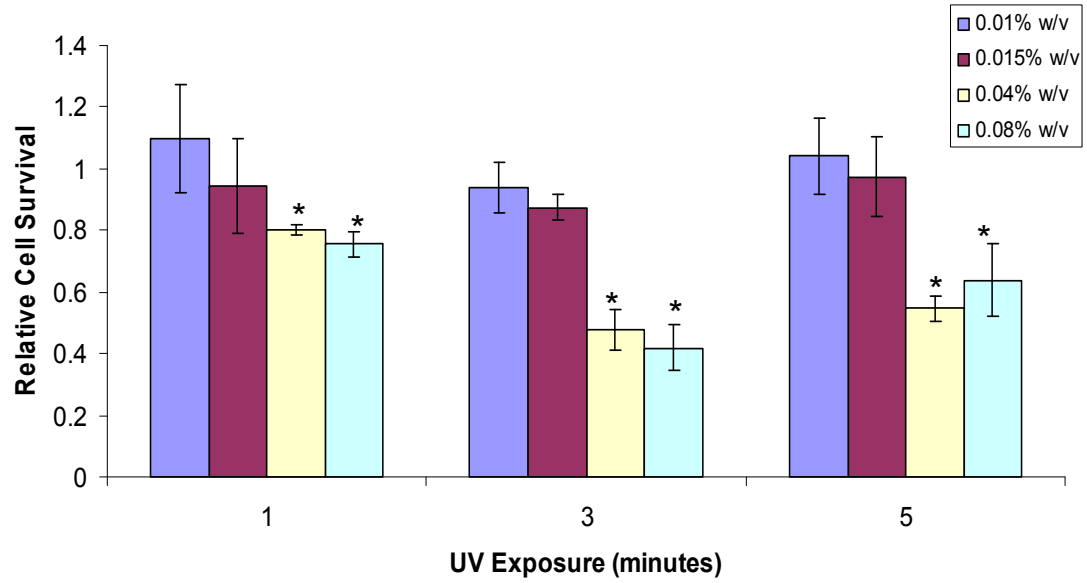

(a)

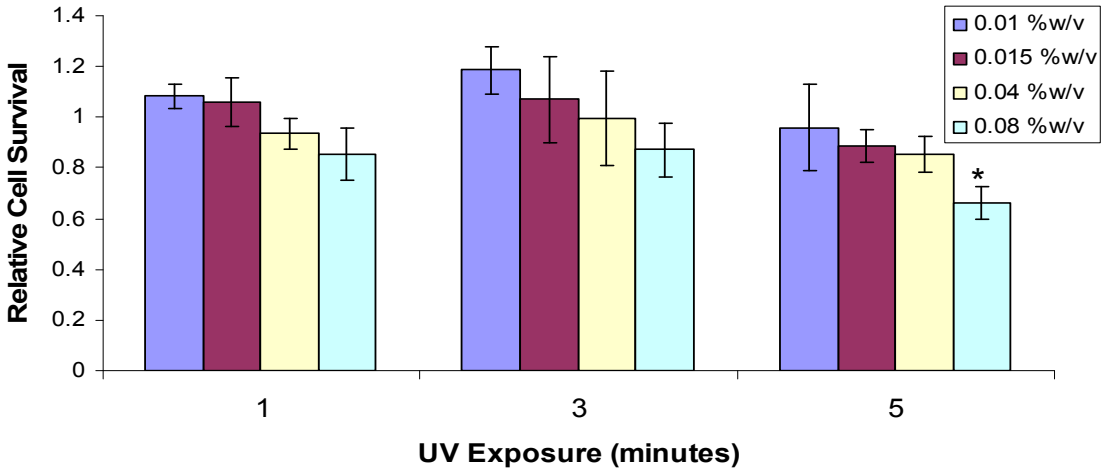

(b)

Figure 2.3 The combined effects of photoinitiator concentrations (0.01%, 0.015%, 0.04%, and 0.08% w/v) and UV exposure (1, 3, and 5 minutes) on the cell survival. (a) Human aortic smooth muscle cells. (b) NIH/3T3 fibroblasts. * = Significant Difference ($p<0.05$)

2.3.4. *Effect of Antioxidant*

To explore methods of reducing cytotoxicity due to the free radicals, a study was carried out to evaluate the efficiency of ascorbic acid, in reducing cellular damage caused by free radicals. HASMCs were incubated in photoinitiator-media solutions supplemented with 50-1000 mg/L of ascorbic acid for 30 minutes before being exposed to UV light. It was observed that even at low concentrations (50 mg/L), ascorbic acid was able to improve the relative cell survival rates by 47% compared to samples without ascorbic acid (Figure 2.4). In addition, a parallel study was carried out to study the effect of antioxidant addition on the gelation time of the hydrogel. Hydrogels with 50 mg/L of ascorbic acid required 50% more time to form when compared to hydrogels with no antioxidant, with all other conditions remaining constant.

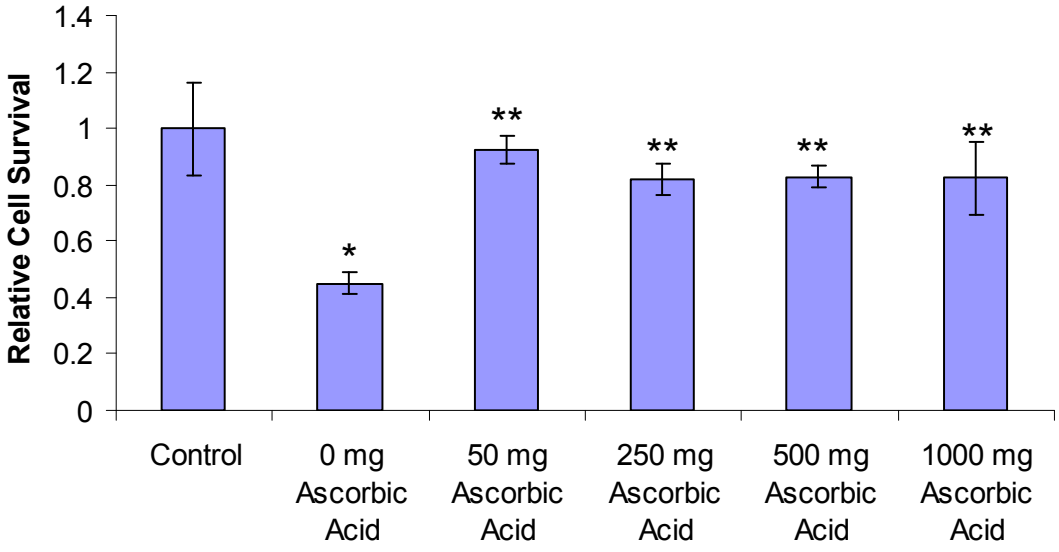

Figure 2.4 Effect of Ascorbic Acid on the HASMC cell survival when exposed to 0.15% (w/v) Irgacure 2959 and 5 minutes of UV exposure. Control was not exposed to photoinitiator and UV light. * = Significant Difference ($p<0.05$) ** = significant difference ($p<0.05$) with respect to 0mg/L Ascorbic acid concentration.

2.4 Discussion

Photopolymerizable hydrogel systems have been used in several applications including drug delivery and tissue engineering. The ability to rapidly form a hydrogel *in situ* using photopolymerization makes this system highly desirable for biomedical applications.[34] In our particular applications, we are developing a thermoresponsive composite nanoparticle hydrogels to aid in wound healing and prevention of restenosis. Following injury or restenosis (and subsequent angioplasty), the hydrogel would be photopolymerized at the injured site to release drugs. It is critical that the drug delivery system components do not cause additional damage on the surrounding cells and tissues. Hence, the aim was to evaluate the cytocompatibility of the components of the photoinitiating system, including the UV light and photoinitiator. HASMCs, normally present at the injured arterial site, were chosen for the evaluation of the cytotoxic effects of the system components for the restenosis application. Similarly for wound healing, fibroblasts which are present at injured skin wound sites were chosen to evaluate the cytotoxicity of the composite system.

Short-time exposure to UV light did not cause significant cytotoxicity as shown in our studies (Figures 2.1) and previous studies from other investigators. Our study, evaluating the cytotoxicity of varying times of UV exposure, showed that UV light did not cause any significant decrease in both HASMC (1.20 ± 0.18) and NIH/3T3 fibroblast (0.90 ± 0.05) survival after 5 minutes of exposure. Similar studies by others conducted on NIH/3T3 fibroblasts cells have shown relative cell survival rates of 1.08 ± 0.03 (n = 2) even after 10 minutes of UV exposure.[29] Williams et al. performed an

extensive study evaluating the effects of UV exposure on six different cell types, including human fetal osteoblasts, bovine chondrocytes, rabbit corneal epithelial cells, human mesenchymal stem cells, goat mesenchymal stem cells, and human embryonic germ cells, and found that short time UV exposure (5 minutes) did not alter cell survival significantly.[31] These results, combined with our data, confirm that while its cytotoxic effects may vary slightly among cell types, UV exposure does not significantly contribute to cell death at conditions (short-time exposure) required for photopolymerization.

Our second study evaluated the effects of different photoinitiator concentrations on the survival of HASMCs and NIH/3T3 fibroblasts (Figure 2.2). It was important to evaluate the cytocompatibility of Irgacure 2959 as these cells would be exposed to the photoinitiator molecules prior to polymerization. Additionally, it is possible that some undissociated photoinitiator molecules could harm the cells after polymerization.[29] Several groups have investigated the cytotoxicity of different, commercially available, visible light and UV photoinitiators.[21,45,48] Williams et al. studied the cytocompatibility of three UV photoinitiators with six different cell lines and found Irgacure 2959 to be the most cytocompatible amongst these six cell lines with different cell types reacting differently to the same concentration of a single photoinitiator.[31] Based on the results from these studies, we selected Irgacure 2959 as a photoinitiator for our composite hydrogel system, and thus, it was important for us to evaluate the cytocompatibility of Irgacure 2959 specific to our cell types. In our study, HASMCs have shown a higher sensitivity to Irgacure 2959 compared to different cell types studied by other groups.

Our results showed that below 0.02% (w/v) concentration, there was no significant decrease in cell survival. At concentrations ≥ 0.02% (w/v), the cytotoxicity of Irgacure 2959 increased with increasing photoinitiator concentrations and significantly affected cell survival. It is also important to note that even low photoinitiator concentrations (0.015%) can photopolymerize the hydrogels within short periods of UV exposure (5 minutes). Additionally, the HASMCs were exposed to Irgacure 2959 for 3 days whereas *in vivo* the cells would be exposed to the photoinitiators for a shorter period. For the fibroblast study, we found Irgacure 2959 to be significantly more cytocompatible with no significant decrease in cell survival even at 0.08% (w/v) concentration. These results are in agreement with previous studies by Bryant et al, which showed Irgacure 2959 did not affect fibroblast survival at concentrations ≤ 0.05% (w/w).[29]

The cellular damage caused by photopolymerization was also evaluated by studying the combined effects of photoinitiator molecules and UV light. It was essential to perform this study as photoinitiator molecules dissociate into free radicals upon exposure to light and can damage cellular membranes.[29] In our studies, at lower photoinitiator concentrations (0.01% and 0.015% w/v) and UV exposure times (1, 3, and 5 minutes), HASMC survival rates were not statistically different from the control (Figure 2.3 a). However, at 0.04% and 0.08% (w/v) photoinitiator concentrations, a significant decrease was noted in HASMC survival rates for all durations of UV exposure. In the fibroblast study (Figure 2.3 b), significant cell death was observed only at 0.08% (w/v) of Irgacure 2959 and 5 minutes of UV exposure, with relative cell

survival being 0.66 ± 0.06 at these conditions. As seen from the HASMC study, for high photoinitiator concentrations, the combined effects of UV and photoinitiator exposure were much higher than the individual effects of each component. This increased cell death can be attributed to the free radicals released during photopolymerization. Following polymerization, cells may also be exposed to a toxic environment consisting of photoinitiator by-products and undissociated photoinitiator molecules in addition to generated free radicals.[29] However, during photopolymerization, the reactive macromers would react with the free radicals, thereby reducing the harmful effects of the radicals on the cells.[31]

Finally we tried to reduce the cytotoxic effects by scavenging the free radicals released during the photopolymerization process. Williams et al. reported that the presence of antioxidant ascorbic acid in the culture media for bovine chondrocytes might have reduced the sensitivity of these cells to the toxic effects of Irgacure 2959.[31] In our study to evaluate the ability of ascorbic acid to scavenge free radicals and reduce photoinitiator toxicity, it was found that ascorbic acid, even at low concentrations (50 mg/L), significantly increased cell survival (Figure 2.4). It was previously reported that different cell types might respond differently to a single photoinitiator due to variations in their expression of antioxidant enzymes,[49] receptors for antioxidant enzymes,[50,51] and the addition of antioxidants to their culture media.[52,53] Our results confirm these findings as we were able to significantly alter cell survival rates by adding an antioxidant. However, it is important to note that free radicals are critical to the polymerization process. Hence, it was necessary to determine whether the presence of

ascorbic acid altered the gelation time of the hydrogel. Our studies showed that upon addition of 50 mg/L concentration of antioxidant ascorbic acid, the time required for gelation increased by 50% compared to the gelation time in the absence of an antioxidant. Although the addition of ascorbic acid significantly improved cell survival, its increased gelation time may result in increased photoinitiator and UV exposure, making ascorbic acid unattractive for use in our system.

2.5 Conclusion

The focus of this chapter was to investigate the cytotoxicity of the photoinitiating components of our composite hydrogel system on human aortic smooth muscle cells and NIH/3T3 fibroblasts. Studies conducted to evaluate the effects of UV dose, photoinitiator concentrations, and combined effects conclusively showed the photoinitiator and free radicals were the most cytotoxic components while UV light did not significantly affect cell survival. Further, the two cell lines were shown to be affected to different degrees by the same photoinitiator concentrations. Additionally, it was shown that ascorbic acid could increase cell survival by 47%, but it also increased the gelation times of the hydrogel by 50%, potentially inducing cellular damage due to prolonged exposure times.

CHAPTER 3

FACTORIAL ANALYSIS

3.1 Introduction

After evaluating the cytotoxicity of the composite hydrogel, it was necessary to optimize the composite system characteristics for two reasons. Firstly, the photoinitiator toxicity imposed certain limits (specific to the cell lines) on the photopolymerization conditions. For instance, lower photoinitiator concentrations must be used for better cell biocompatibility; however, low photoinitiator would increase gelation times. Secondly, in our system, the thermoresponsive drug-loaded nanoparticles are entrapped within the PEGDA hydrogel network. Therefore the drug release from the composite system is governed by diffusion of drug through this network. The components of our composite system that can affect the network structure and characteristics (and thus drug release) include the PEGDA cross-linker and PNIPA-AAm nanoparticles. This made it necessary to evaluate the effect of factors such as PEGDA molecular weight and concentration as well as the amount of PNIPA-AAm nanoparticles on the gelation times, drug release profiles and swelling ratios.

It was expected that low MW PEGDA networks may contain shorter cross-linker chains and may result in a denser and more compact network by forming shorter cross-links. This compact network might impede the drug diffusion from the network. Alternatively, high MW PEGDA networks would form looser and more flexible

networks, thus allowing better diffusion of released drug. With respect to PEGDA concentrations, our hypothesis was that a high concentration of cross-linker would result in a tighter network due to the increased number of PEGDA chains. This, in turn, would result in lower release of drug from the composite system. Finally, an increased amount of drug-loaded PNIPA-AAm nanoparticles entrapped within the hydrogel network would theoretically translate into a higher drug release. However, it remains to be seen to what extent this drug release would be impeded or aided by the other factors, namely, PEGDA MW and concentration.

Hence the aim of the factorial analysis study was to investigate the system characteristics, such as gelation time, drug release and swelling ratio, in response to changes in the 3 factors (PEGDA MW, PEGDA concentration and PNIPA-AAm nanoparticle concentration) using a standard factorial design method. Different combinations of high and low levels of the 3 factors were selected based on the factorial design, and half-factorial model was selected was analysis of our system. The responses were then determined experimentally and the collected data was analyzed to evaluate the individual effects of the 3 factors on the composite system behavior.

3.2 Materials and Methods

3.2.1. Preparation of Poly(ethylene glycol diacrylate) (PEGDA)

Factorial design of our hydrogel system required evaluation of two molecular weights (MW) (3.4 kDa and 8 kDa) of the cross-linker, PEGDA. PEGDA was synthesized by modifying the previously described methods.[54,55] Briefly, 12 grams of

poly(ethylene glycol) (3.4 kDa or 8 kDa) was dissolved in 36 ml of anhydrous dichloromethane. 1.3 ml of triethylamine (TEA) was added to the flask and the solution was bubbled with argon gas for 5 minutes. 0.61 ml of Acryloyl chloride (AC) was then dissolved in 10 ml of dichloromethane and added dropwise slowly (over an hour) to the flask on ice. The solution was stirred under argon for 2 days on an ice bath. After stirring, the solution was washed with 2M K_2CO_3 to separate the dichloromethane phase, followed by drying with anhydrous $MgSO_4$. PEGDA was then precipitated using ethyl ether.. Finally the product was filtered and dried for 12 hours under vacuum at room temperature.

3.2.2. Factorial Analysis using Design of Experiments

Our factorial studies utilized design of experiments (DOE) to minimize the number of runs required to elucidate the effect of individual factors on the hydrogel system. Using DOE, it was possible to design a half-factorial experiment (4 instead of 8 runs) for 3 factors with 2 levels. The 3 factors (independent variables) included the PEGDA MW (3.4 kDa, 8 kDa) and concentration (10%, 15% w/v) and PNIPA-AAm nanoparticle concentration (2%, 4% w/v). The evaluated responses (dependent variables) were included the gelation time, drug release (25^oC versus 40^oC) and the swelling ratio of the hydrogels. According to the half-factorial design, 4 runs were chosen by splitting the full 3-factor 8-run design to accurately evaluate the effects of the 3 factors by halving the number of experimental runs. The resulting factorial design is shown below. PEGDA MW, concentration and PNIPA-AAm nanoparticle

concentration have been represented as M, P and N respectively. The experiments were performed based on the factorial design and the data collected was analyzed to evaluate the effect on the responses as the factors changed from low to high levels.

Table 3.1 Low and High Levels for the Half Factorial Design

Level	M (Da)	P (% w/v)	N (% w/v)
Low (0)	3.4 k	10	2
High (1)	8 k	15	4

Table 3.2 Coded Values of the Half Factorial Design

Run #	M (Da)	P (% w/v)	N (% w/v)
1	0	0	0
2	1	0	1
3	1	1	0
4	0	1	1

Table 3.3 Actual Values of the Half Factorial Design

Run #	M (Da)	P (% w/v)	N (% w/v)
1	3.4 k	10	2
2	8 k	10	4
3	8 k	15	2
4	3.4 k	15	4

3.2.3. Preparation of Photopolymerized Thermoresponsive Hydrogels

PNIPA-AAm nanoparticles were prepared as previously described in section 2.2.6. The nanoparticles were then dispersed in deionized water to get a 5% (w/v) stock suspension. Bovine serum albumin (BSA), as a model protein, was added to the stock suspension at a concentration of 5% (w/v) and incubated at $4^{o}C$ for 4 days. The photoinitiator solution consisting of 0.125 g of Irgacure 2959 in 10 ml PBS was then prepared and protected from light. Hydrogels (n=4) for the factorial analysis were prepared based on the table 3.3. For example, run 1 was prepared by dissolving 0.1 g of PEGDA (3.4 kDa) in 400 µl of BSA-loaded PNIPA-AAm nanoparticle suspension and 400 µl of PBS. 200 µl of the photoinitiator stock solution was finally added to this solution to make 1 ml total solution with final PEGDA and PNIPA-AAm nanoparticle concentrations of 10% (w/v) and 2% (w/v), respectively. To form the hydrogel, 200 µl of the precursor solution was added to a 48-well plate and exposed to UV light at about 10 mW/cm^2.

3.2.4. Effects on Gelation Time

The time taken to form the hydrogels, i.e. gelation time, was measured to evaluate its dependence on the factors. For each run, 4 hydrogels were photopolymerized and an average gelation time value for these hydrogels was calculated, following which the factorial analysis was carried out.

3.2.5. Effects on Drug Release

To evaluate the effect of the factors on drug release, protein loaded nanoparticle hydrogels (n=4) for each run were incubated at room temperature (25^{o}C) and LCST (40^{o}C) in 24-well plates with 1 ml of PBS solution. At the pre-determined time points (1, 2, 4, 8, 12, 24 and 48 hours), the PBS solution from the wells was replaced with 1 ml of fresh PBS solution. The samples collected at various time points were then analyzed using the BCA protein assay (Pierce, following manufacturer's instructions) to evaluate the amount of protein released from the hydrogel. The data was analyzed and the drug release profiles for each run at 25^{o}C and 40^{o}C were plotted.

3.2.6. Effects on Swelling Ratio

The swelling ratios for the hydrogels from different runs were determined to better understand how the factors such as PEGDA MW and concentration as well as PNIPA-AAm nanoparticle concentration affected the hydrogel structure. After photopolymerization, the hydrogels (n=4) were allowed to swell with PBS solution at room temperature for 4 days. These swollen hydrogels were then dried with moistened filter paper and weighed to get the W_S, the swollen weight of the hydrogels. The dry weight of the hydrogels, W_D, was calculated after allowing the hydrogels to dry at room temperature for 4 days followed by weight measurement.

The swelling ratio (S.R.) of the hydrogels was calculated using the equation 3.1.

$$S.R. = \frac{W_S - W_D}{W_D} \tag{3.1}$$

3.3 Results

3.3.1. Effects on Gelation Time

Hydrogels were formed according to the half-factorial design (Table 3.3) and for each run, the average gelation time was measured (Table 3.4). Using factorial analysis, the effect of each factor (at low and high level) on gelation time was evaluated. The results of study showed that the gelation time was reduced by varying degrees as each factor changed from low to high levels (Figure 3.1). Each factor exhibited an inverse relationship to the gelation time, i.e. as the factor level changed from low to high, the gelation time reduced. However maximum reduction in gelation time (21.44 seconds) was observed as the PEGDA concentration changed from 10% to 15% (w/v). As PEGDA MW changed from 3.4 kDa to 8kDa, the gelation time reduced by 11.56 seconds while changing PNIPA-AAm nanoparticle concentrations from 2% to 4% (w/v) resulted in 10.44 seconds reduction in gelation time. Thus our results showed that PEGDA concentration was the single most important factor in determining the gelation time of our composite hydrogels.

Table 3.4 Effects of Factors on Gelation Time.

Run #	M (Da)	P (% w/v)	N (% w/v)	Gelation Time (seconds)
1	3.4 k	10	2	118.5
2	8 k	10	4	96.5
3	8 k	15	2	85.5
4	3.4 k	15	4	86.625

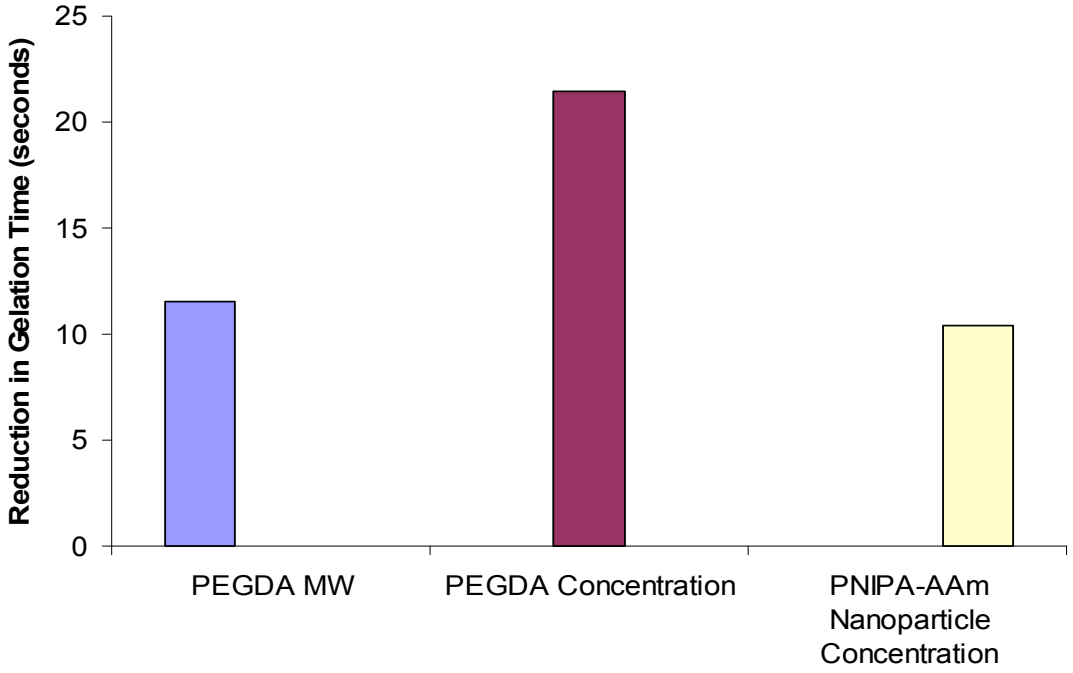

Figure 3.1 The effects on gelation time as the 3 factors are changed from low to high level.

Figure 3.2 (a) and (b) show the variations in gelation time as a function of PEGDA MW and PNIPA-AAm nanoparticle concentration at low and high levels of the most significant factor, PEGDA concentration.

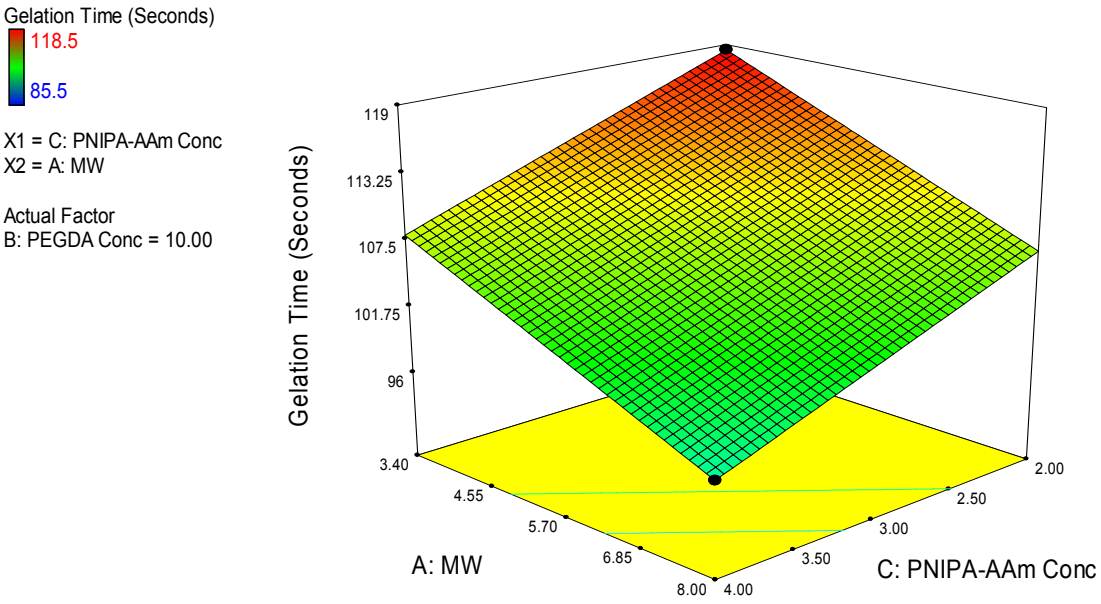

(a)

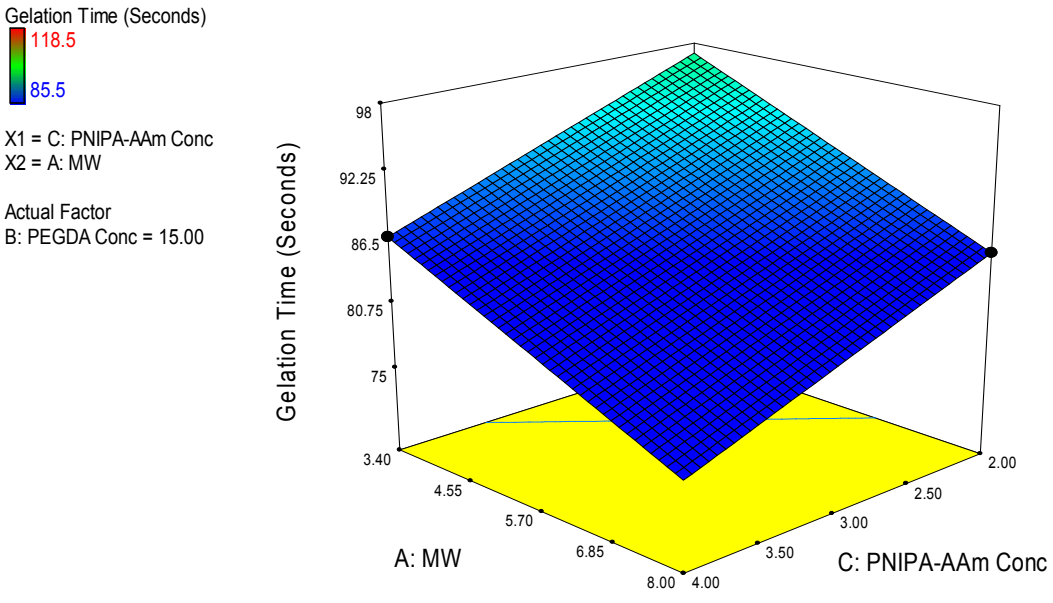

(b)

Figure 3.2 Variation in gelation time with (a) 10% (w/v) and (b) 15% (w/v) PEGDA concentration.

3.3.2. Effects on Drug Release

To evaluate the effect of the factors on the drug release and thermoresponsive behavior of the hydrogel composite system, the drug release study was performed. The cumulative protein release for different runs was plotted to represent the drug release profiles at 25°C and 40°C (Figure 3.3).

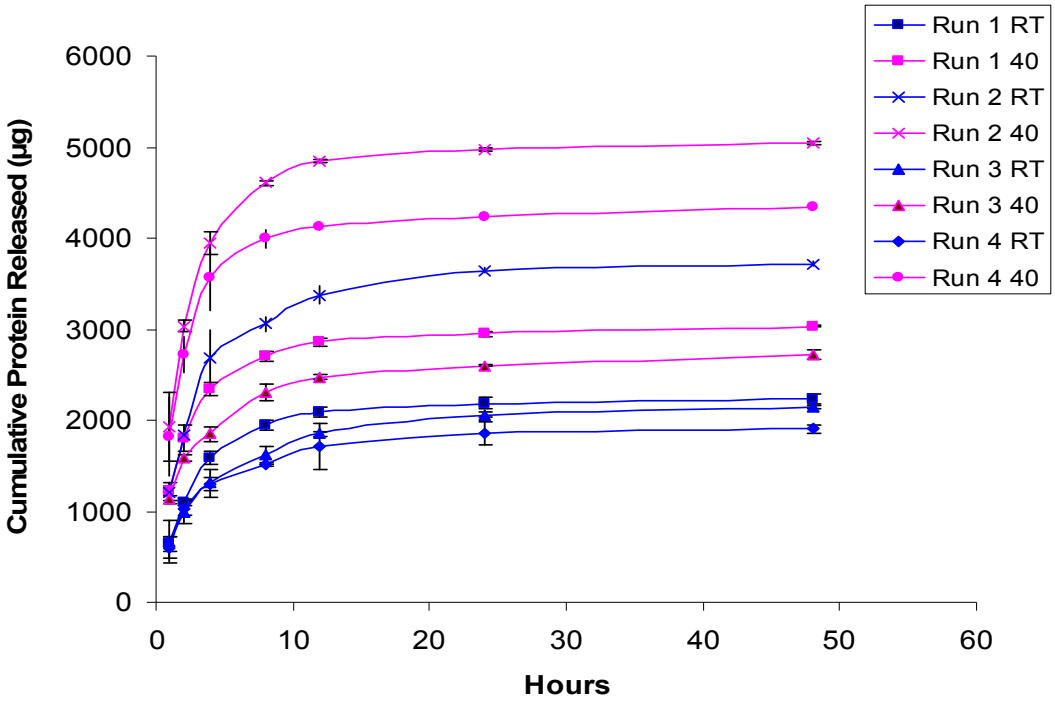

Figure 3.3 Cumulative drug release profiles of the different composite hydrogels as an effect of the 3 factors. RT= 25°C; 40=40°C

The drug release profiles from the different runs were also plotted individually to better visualize the thermoresponsive behavior of the hydrogels (Figures 3.4).

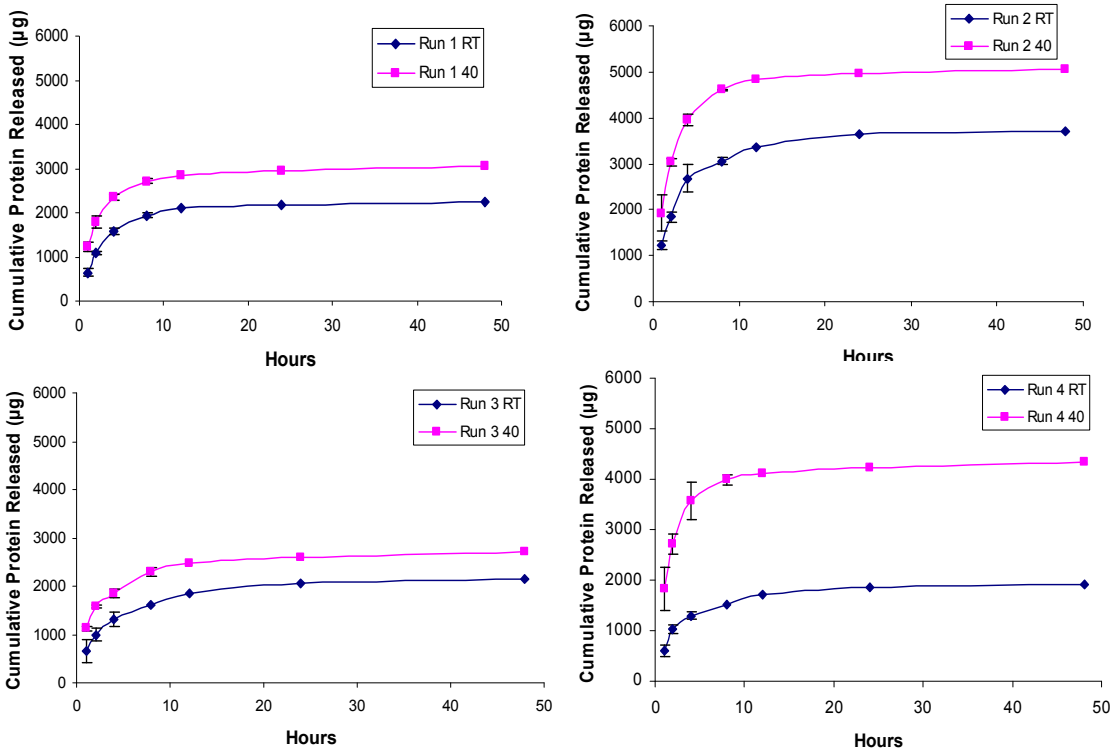

Figure 3.4 Drug release profiles at 25°C and 40°C

From the drug release profiles above, it can be observed that all runs showed a biphasic drug release, with an initial burst release (up to 8 hours) followed by a plateau release (up to 48 hours). Most of the protein was released within the first 8 hours of the release study. In addition, all 4 runs showed a thermoresponsive release behavior with hydrogels at 40°C releasing a significantly higher amount of protein as compared to hydrogels at 25°C, over the same time duration. Hydrogels from run 2 showed the highest cumulative drug release among the 4 different runs, followed by run 4. Runs 1 and 3 showed the lowest drug release among the runs.

3.3.2.1 Dependence of Drug Release on Factors

To better understand which factors governed the drug release characteristics from the hydrogels, the drug release rates were calculated for the different runs at both temperatures (Figure 3.5). Drug release rates were calculated by using equation 3.2.

$$\text{Drug Release Rate, } R = \frac{D_2 - D_1}{t_2 - t_1} \tag{3.2}$$

Where:

R is the drug release rate between two time points (μg/hr)

D_1, D_2 are amounts of drug released at time t_1 and t_2 respectively (μg)

t_1, t_2 are time points at which drug release was quantified (hours)

Table 3.5 Drug Release Rates at t_1 = 0 hours and t_2 = 48 hours

Run #	M (Da)	P (% w/v)	N (% w/v)	Release Rate 25°C (μg/hr)	Release Rate 40°C (μg/hr)
1	3.4 k	10	2	46.523	63.232
2	8 k	10	4	77.383	105.191
3	8 k	15	2	44.679	56.676
4	3.4 k	15	4	39.732	90.282

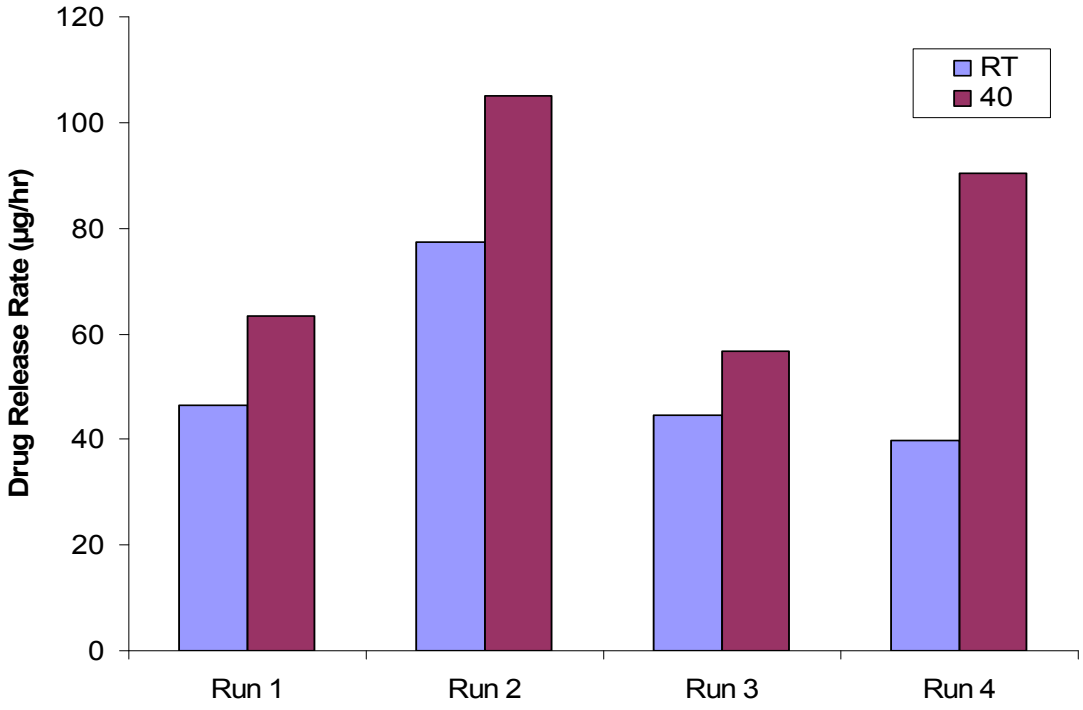

Figure 3.5 Drug release rates for different hydrogels (Run 1-4) at 25°C and 40°C.

At both temperatures, drug release rates calculated for all runs with t_1=0 hours and t_2=48 hours are shown in table 3.5 and figure 3.5. Using the release rate values, a factorial analysis was performed to evaluate the effect of individual factors on drug release profiles. At 25°C, it was observed that changing PEGDA MW and PNIPA-AAM nanoparticle concentration from low to high levels had positive effects on the drug release rate, i.e. these factors increased the drug release (Figure 3.6). However, changing the PEGDA concentration from 10% to 15% (w/v) actually reduced the drug release rate significantly. Increasing PEGDA molecular weight to 8 kDa was found to increase the drug release rate by 17.9 µg/hr while increasing PNIPA-AAm nanoparticle concentration to 4% (w/v) resulted in an increase of 12.4 µg/hr. On the other hand,

PEGDA concentration reduced the drug release rate by 19.75 µg/hr. Thus, from the factorial analysis it was possible to conclude that PEGDA MW and concentration were the most important factors in increasing and reducing the drug release rate, respectively.

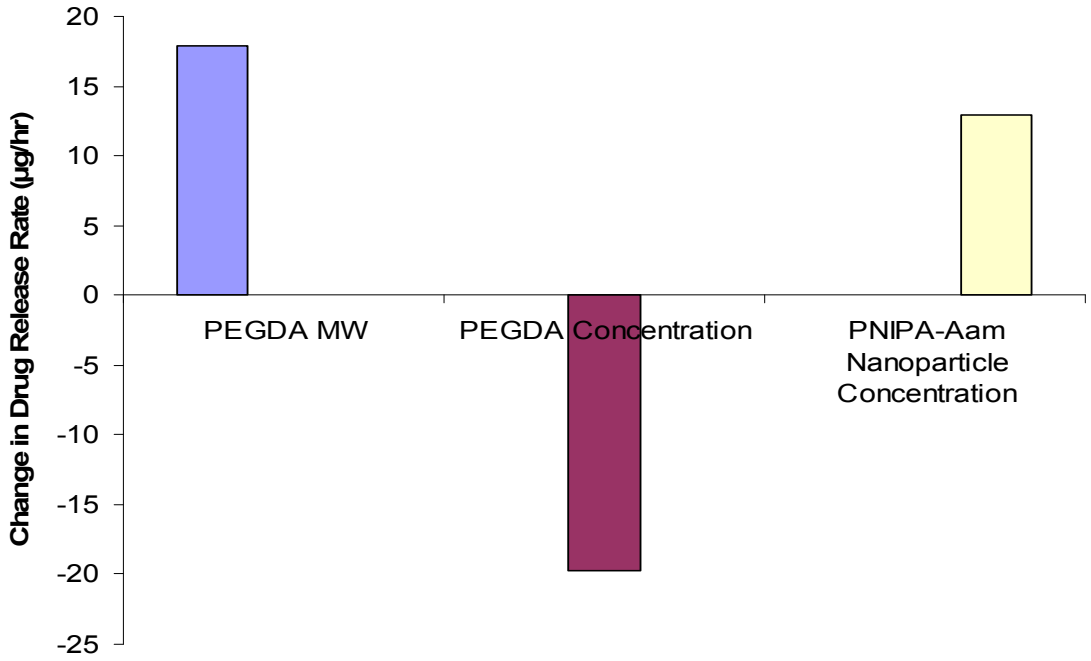

Figure 3.6 Effect of factors on drug release rates at 25°C.

Figures 3.7 (a) and (b) show the variations in drug release rates at 25°C as a function of PEGDA MW and PNIPA-AAm nanoparticle concentration at low and high levels of the most significant factor, PEGDA concentration.

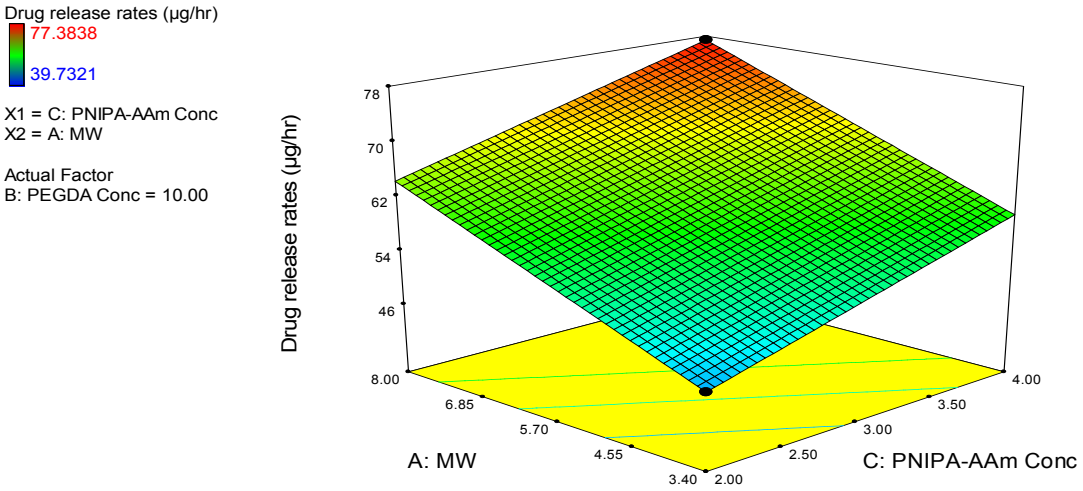

(a)

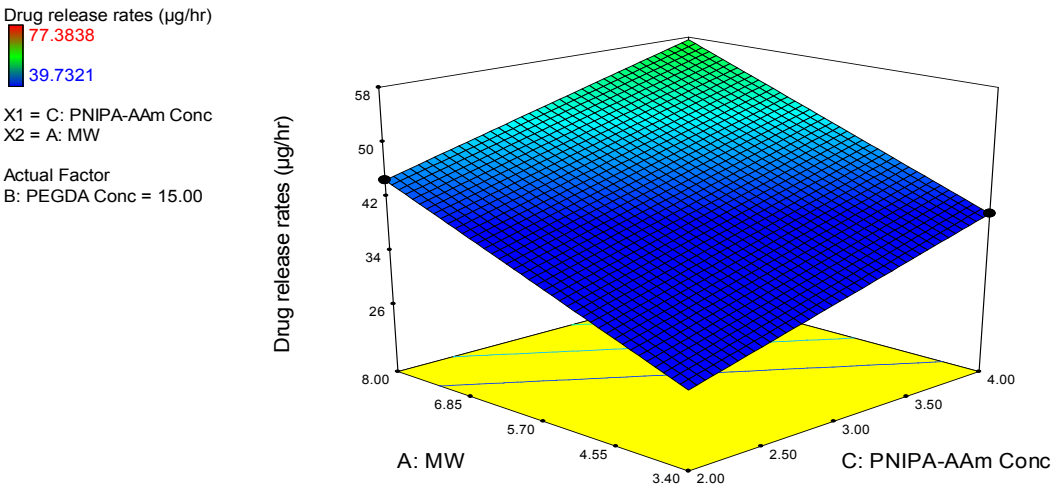

(b)

Figure 3.7 Variation in drug release rate at 25°C with (a) 10% (w/v) and (b) 15% (w/v) PEGDA concentration.

At 40°C, however, PNIPA-AAm nanoparticle concentration was the most important factor and increased the drug release rate by 37.78 µg/hr as compared to PEGDA MW which only increased the release rate by 4.18 µg/hr (Figure 3.8). PEGDA concentration still caused a reduction of 10.73 µg/hr in the release rate when its

concentration increased from 10% to 15% (w/v). Contrary to 25°C, the PNIPA-AAm nanoparticle concentration was the most significant factor affecting the drug release rate at 40°C.

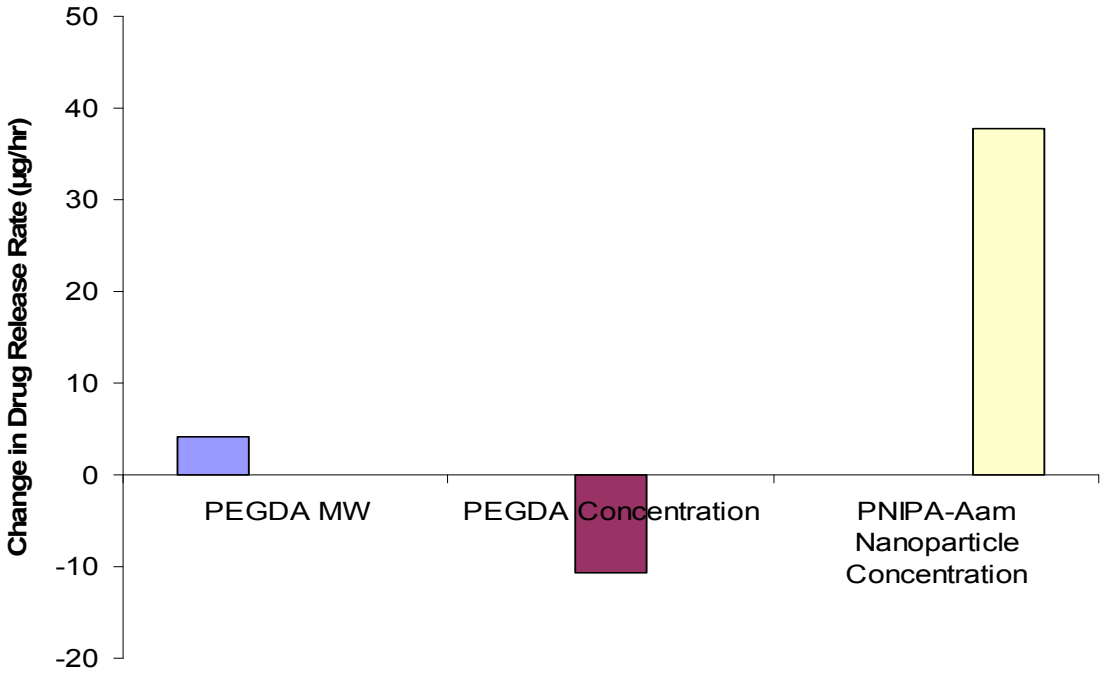

Figure 3.8 Effect of factors on drug release rates at 40°C.

Figures 3.9 (a) and (b) show the variation in drug release rates at 40°C as a function of PEGDA MW and PEGDA concentration at low and high levels of the most significant factor, PNIPA-AAm nanoparticle concentration.

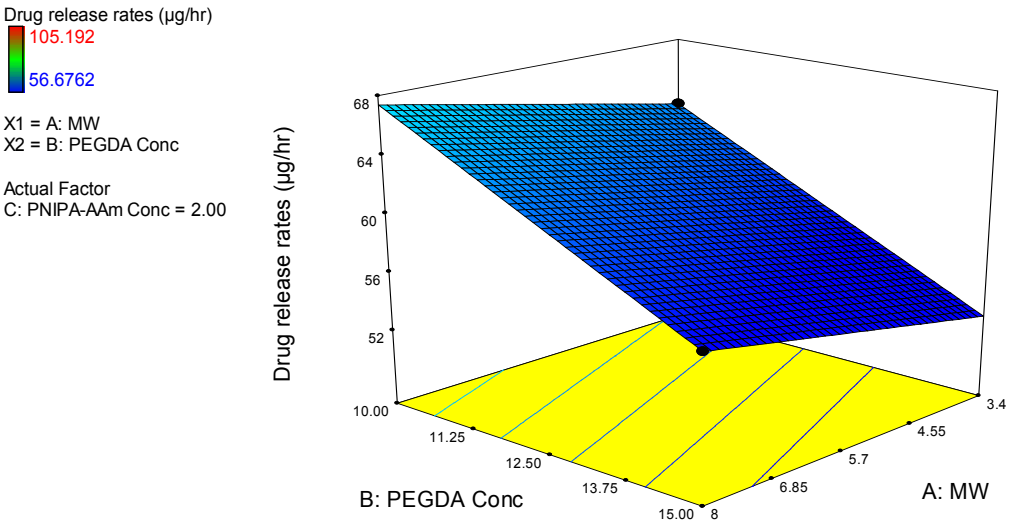

(a)

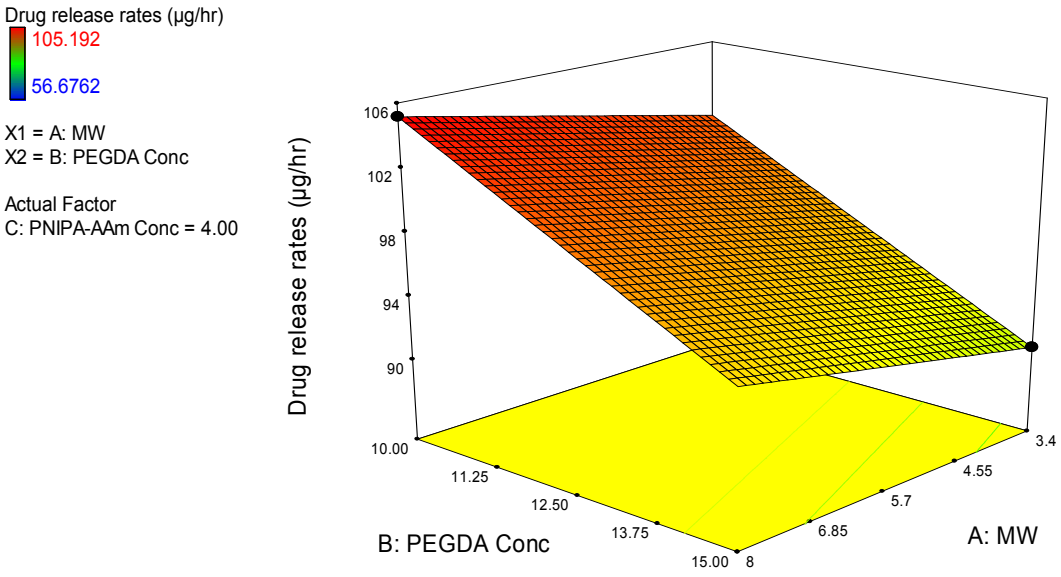

(b)

Figure 3.9 Variation in drug release rate at 40^{o}C with (a) 2% (w/v) and (b) 4% (w/v) PNIPA-AAm nanoparticle concentration.

Analyzing the drug release rates gave us an idea of how different factors affected the drug release at 40°C over the duration of drug release study (48 hours). However, as seen from figure 3.3, the drug release is biphasic and exhibits an initial burst release in which most of the protein is released during the first 8 hours. Hence, it was important to evaluate the release dynamics over two periods, namely, 0 to 8 hours and 8 to 48 hours. The drug release rates at 40°C for these two periods were then calculated and analyzed for factorial influence. Since the drug release will occur in the body temperature range, only the drug release at 40°C was further analyzed.

Table 3.6 Drug Release Rates at 40°C

Run #	M (Da)	P (% w/v)	N (% w/v)	Release Rate (μg/hr) t_1 = 0 hrs, t_2 = 8 hrs	Release Rate (μg/hr) t_1 = 8 hrs, t_2 = 48 hrs
1	3.4 k	10	2	338.567	8.165
2	8 k	10	4	575.833	11.063
3	8 k	15	2	287.552	10.501
4	3.4 k	15	4	499.140	8.511

At t_1 = 0 hr and t_2 = 8 hrs (Figure 3.10), it can be seen that run 2 showed the highest drug release rate, followed by run 4. Runs 1 and 3 showed lower yet similar drug release rates over 8 hours. The influence of the factors on the early drug release (0-8 hours) was then analyzed and shown in figure 3.11. It was observed that at 8 hours, an increase in PNIPA-AAm nanoparticle concentration resulted in a 224.42 μg/hr increase in drug release rate and was the single most important factor governing drug

release. PEGDA MW changes affected the drug release rate positively (12.83 μg/hr) while PEGDA concentration changes reduced the release rate by 63.85 μg/hr.

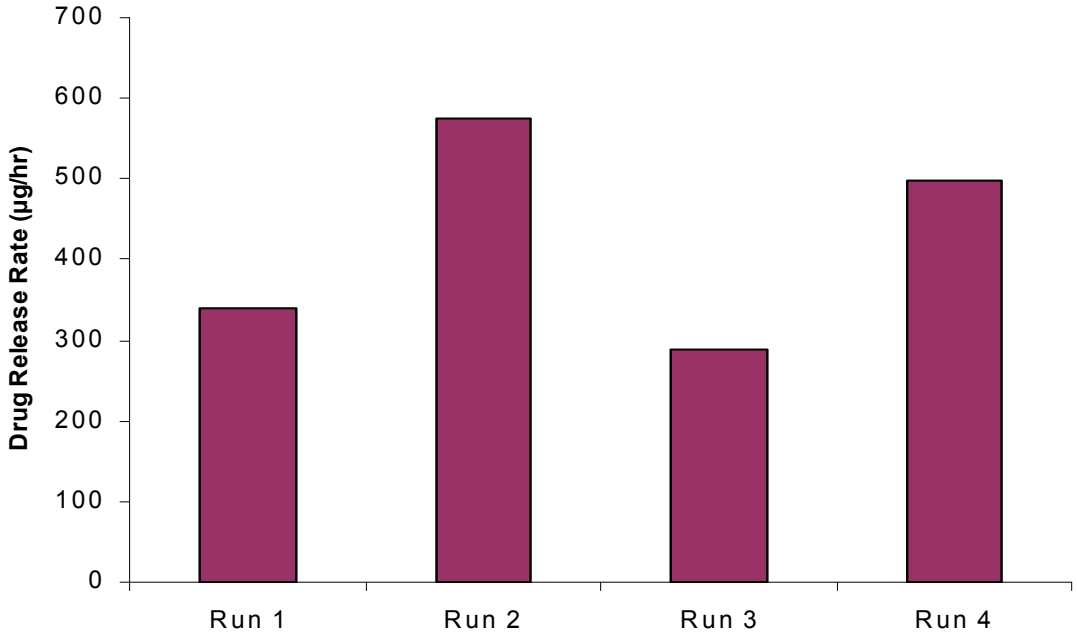

Figure 3.10 Drug release rates at 40°C for t_1 = 0 hrs and t_2 = 8 hrs.

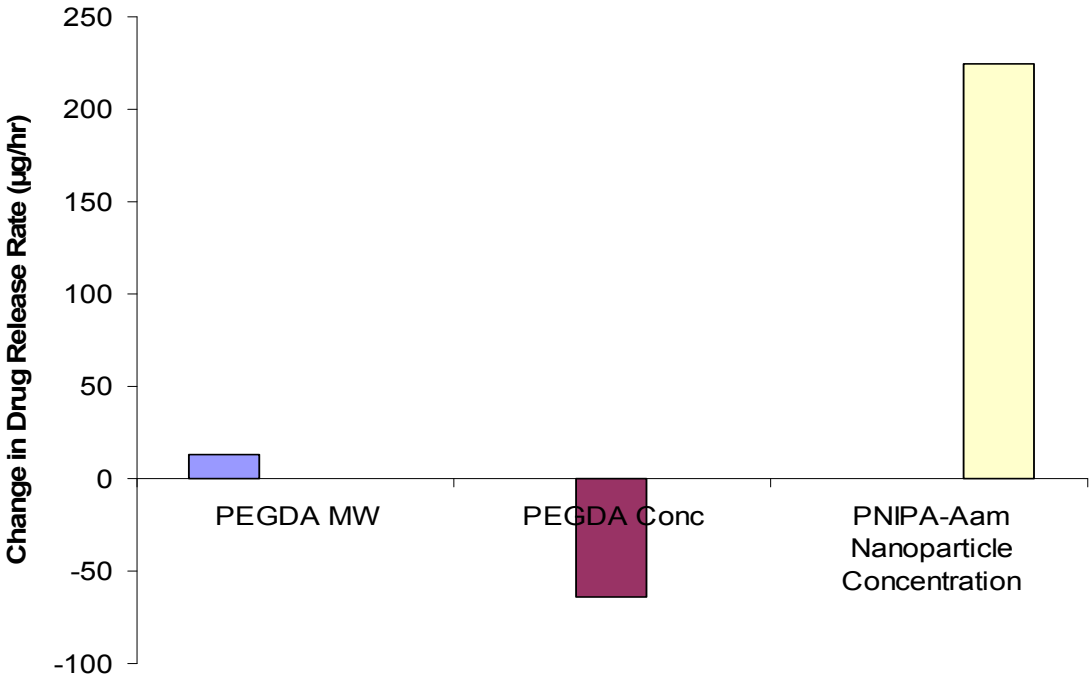

Figure 3.11 Effect of factors on the drug release rates at 40°C for t_1 = 0 hrs and t_2 = 8 hrs.

Figures 3.12 (a) and (b) show the variation in drug release rates at 40°C (t_1 = 0 hrs and t_2 = 8 hrs) as a function of PEGDA MW and PEGDA concentration at low and high levels of the most significant factor, PNIPA-AAm nanoparticle concentration.

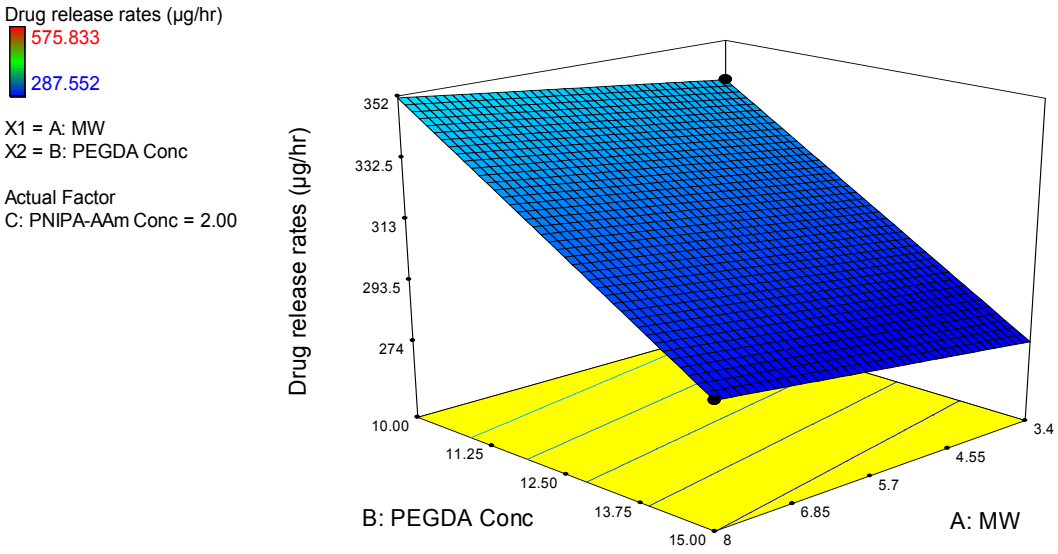

(a)

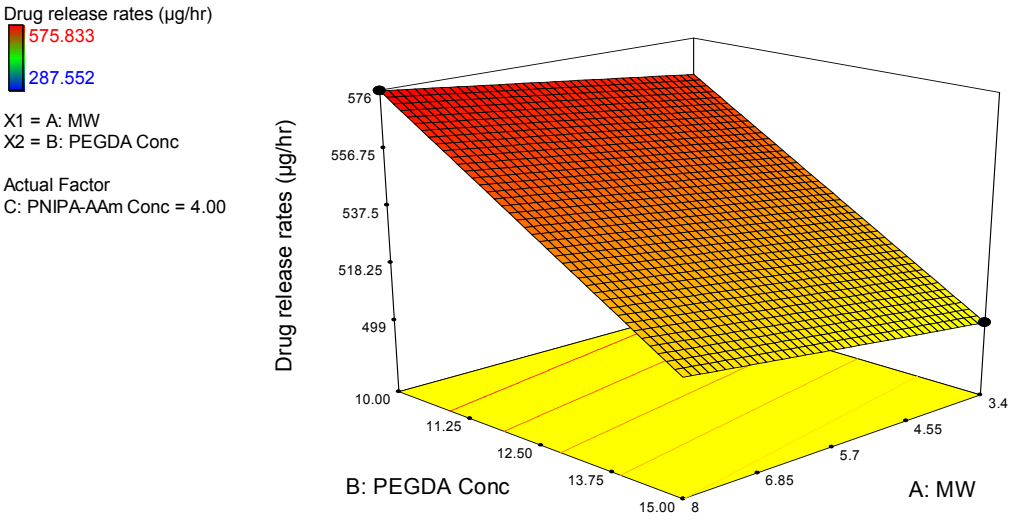

(b)

Figure 3.12 Variation in drug release rate at 40°C with (a) 2% (w/v) and (b) 4% (w/v) PNIPA-AAm nanoparticle concentration. (t_1 = 0 hrs and t_2 = 8 hrs)

The drug release rates between 8 and 48 hours are shown in Figure 3.13. The factorial analysis revealed that PEGDA MW was the major factor governing drug release during the plateau release phase, i.e. 8 to 48 hours, and changed the release rate by 2.44 μg/hr (Figure 3.14). PNIPA-AAm nanoparticle concentration (0.454 μg/hr) had a small positive effect on the release rate while PEGDA concentration (0.10 μg/hr) negligibly reduced the release rate.

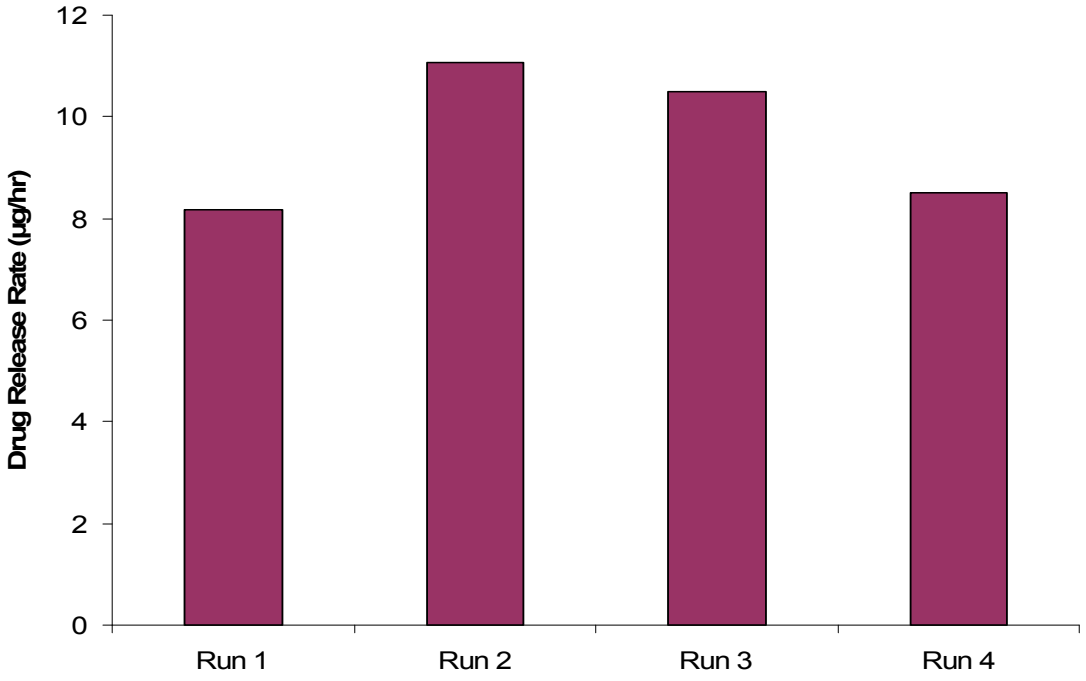

Figure 3.13 Drug release rates at 40°C for t_1 = 8 hrs and t_2 = 48 hrs.

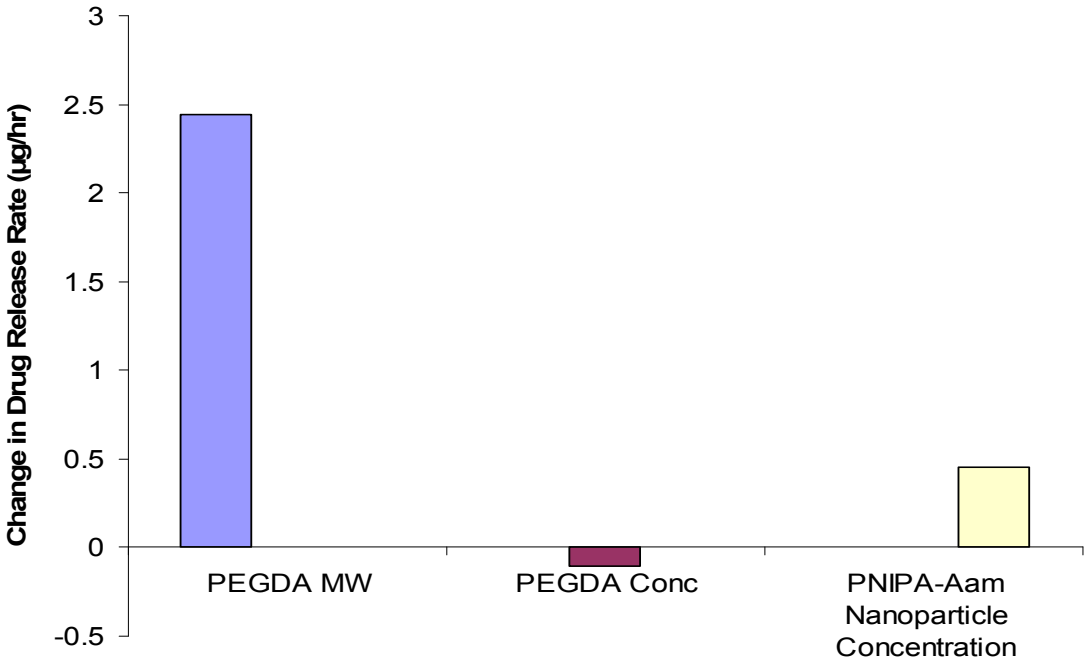

Figure 3.14 Effect of factors on the drug release rates at 40°C for t_1 = 8 hrs and t_2 = 48 hrs.

Figures 3.15 (a) and (b) show the variation in drug release rates at 40°C (t_1 = 8 hrs and t_2 = 48 hrs) as a function of PNIPA-AAm nanoparticle concentration and PEGDA concentration at low and high levels of the most significant factor, PEGDA MW.

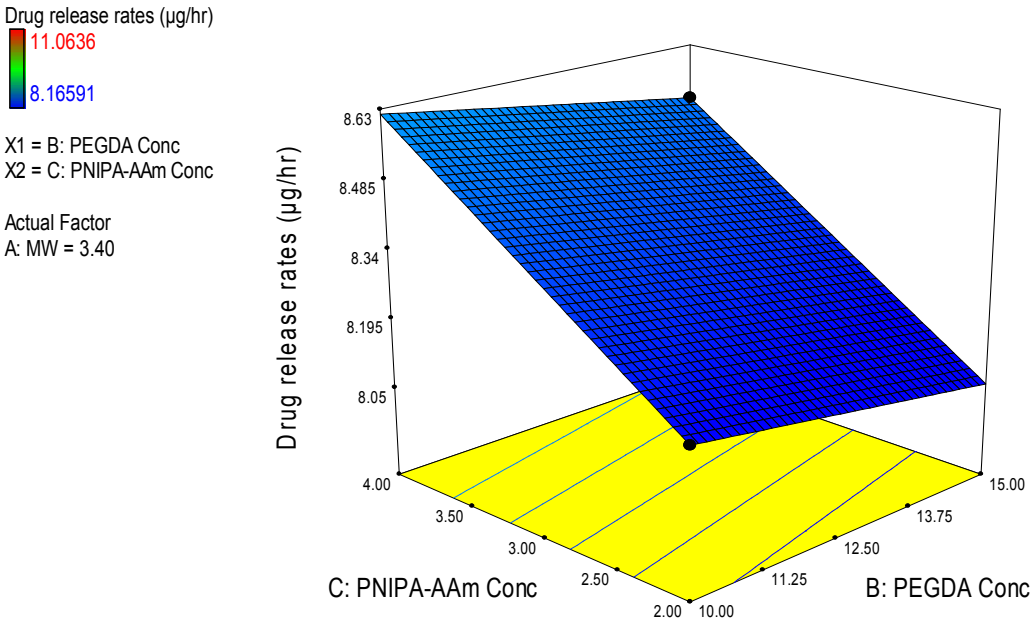

(a)

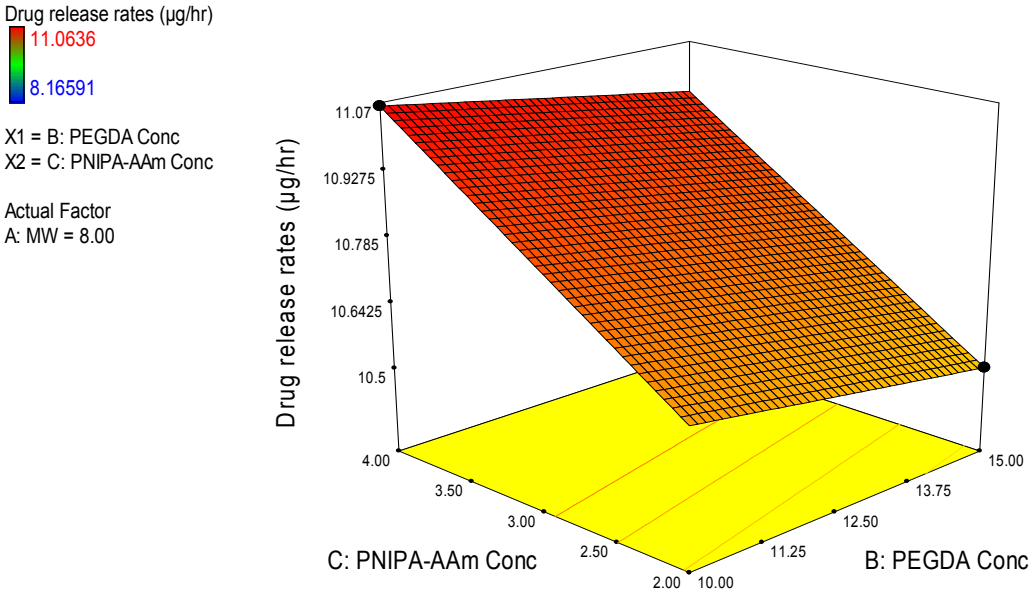

(b)

Figure 3.15 Variation in drug release rate at 40^{o}C with (a) 3.4 kDa and (b) 8 kDa MW PEGDA (t_1 = 8 hrs and t_2 = 48 hrs).

3.3.2.2 Dependence of Thermoresponsiveness on Factors

One of the main reasons to perform the factorial analysis on the photopolymerized hydrogel composite systems was to elucidate the relationship between the factors and the hydrogel thermoresponsive behavior, i.e. higher drug release at 40^{o}C than at 25^{o}C. From figure 3.3, it is clear that all four runs showed a significant thermoresponsive behavior. However, from figure 3.5, the difference in the drug release for all runs is not constant, i.e. all runs do not show the same degree of thermoresponsive behavior. To better understand this effect, the release rate difference (up to 8 hours) between 25^{o}C and 40^{o}C (Figure 3.16) for all four runs was plotted to show the degree of thermoresponsiveness. Release rates differences were only measured from 0 to 8 hours since most of the thermoresponsive behavior was observed within this time period.

It is interesting to note that run 4 showed a greater degree of thermoresponsive behavior compared to other runs, with a release difference of 310.93 μg/hr between the two temperatures (Figure 3.16). Additionally, run 2 showed a difference of 193.1 μg/hr whereas runs 1 and 3 showed a difference of 95 μg/hr and 84.75 μg/hr respectively. On analyzing the factorial influence on the thermoresponsive behavior, changing PNIPA-AAm nanoparticle concentration to the high level was found to result in a 161.639 μg/hr increase in thermoresponsive behavior (Figure 3.17). Interestingly, PEGDA concentration was found to have a positive effect on the thermoresponsive behavior and showed an effect of 53.29 μg/hr. Finally, changing from 3.4 kDa to 8 kDa MW PEGDA resulted in a reduction of 64.54 μg/hr in the thermoresponsive behavior.

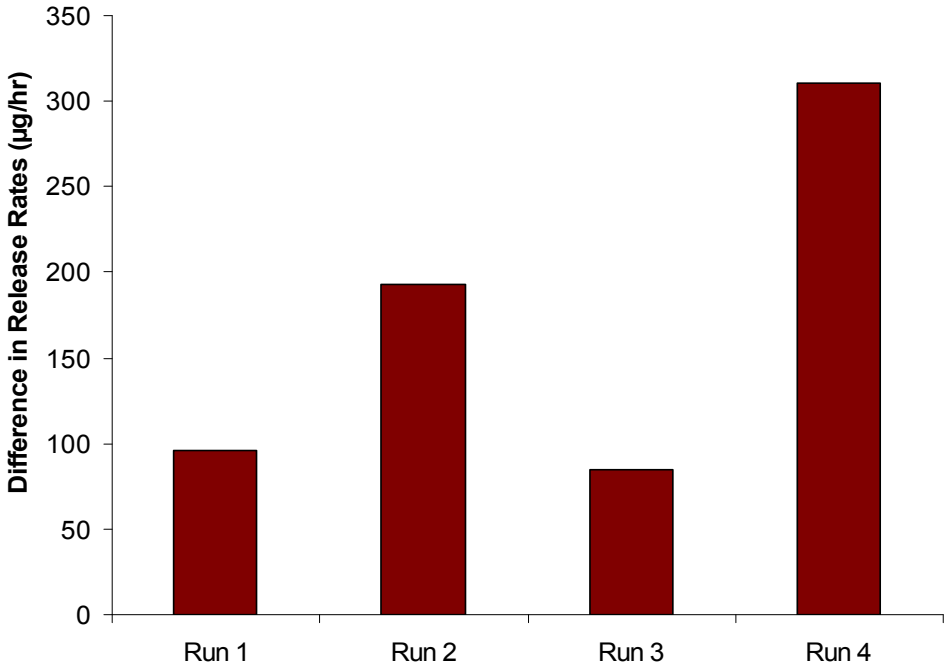

Figure 3.16 Difference between the drug release rates at 25°C and 40°C for the four hydrogel runs (up to 8 hrs).

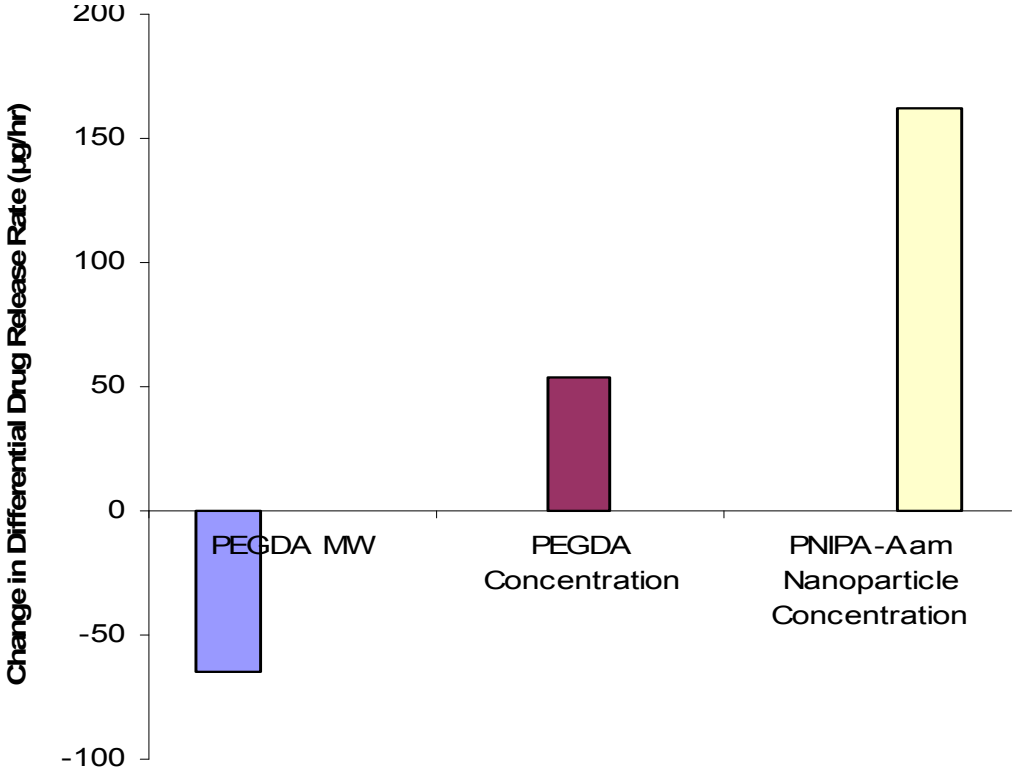

Figure 3.17 Effect of the factors on the thermoresponsiveness of the 4 hydrogel runs (up to 8 hrs).

Figures 3.18 (a) and (b) show the variations in difference between drug release rates at 25°C and 40°C (up to 8 hrs) as a function of PEGDA MW and PEGDA concentration at low and high levels of the most significant factor, PNIPA-AAm nanoparticle concentration.

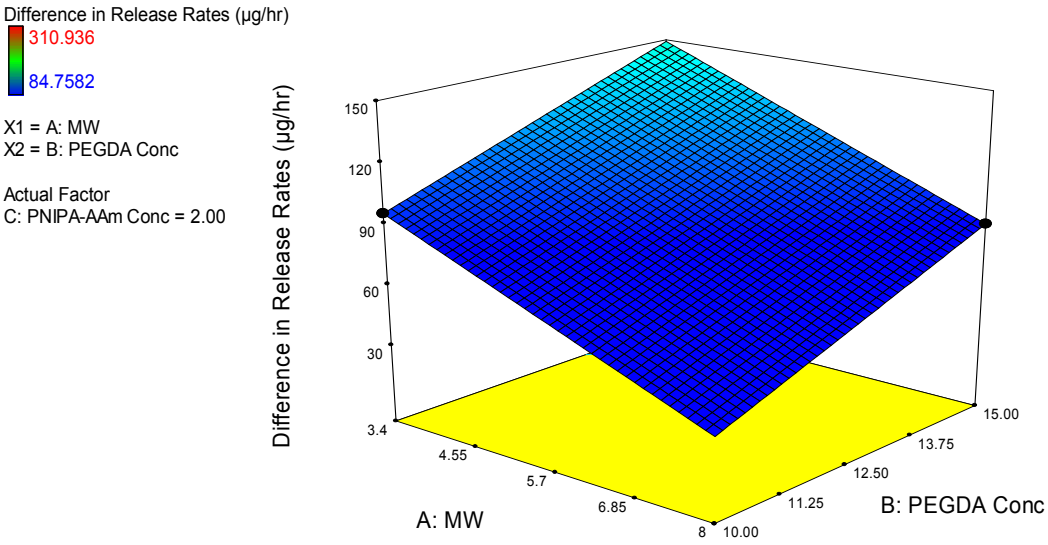

(a)

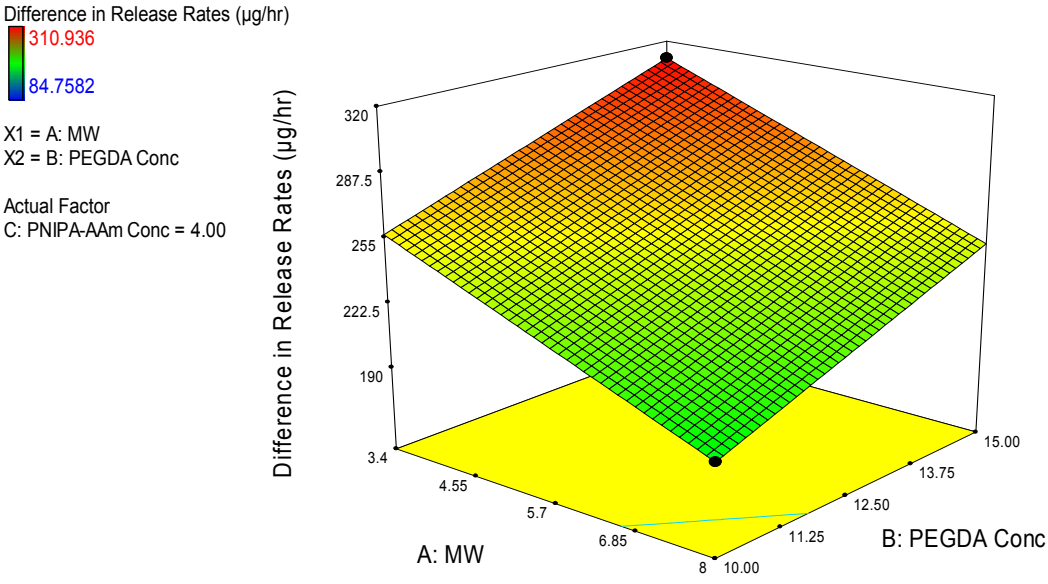

(b)

Figure 3.18 Variation in difference between drug release rates at 25°C and 40°C with (a) 2% (w/v) and (b) 4% (w/v) PNIPA-AAm nanoparticle concentration (t_1 = 0 hrs and t_2 = 8 hrs).

3.3.3. Effects on Swelling Ratio

To evaluate the effects of the factors on the swelling ratio, the swollen weights (W_S) and dry weights (W_D) of the hydrogels (n=4) were measured. The swelling ratios of the hydrogels were then calculated using the equation 3.1 (Table 3.7). A factorial analysis was then performed to recognize the factors responsible for affecting the swelling ratios of the hydrogels (Figure 3.19). The factorial analysis on the hydrogel swelling ratio revealed that increasing the PEGDA MW from 3.4 kDa to 8 kDa was the most important factor in increasing the swelling ratio. Changes in PEGDA MW increased the swelling ratio by 13.62. On the other hand, changing both PEGDA concentration and PNIPA-AAm nanoparticle concentration to the high levels reduced the swelling ratio by 4.59 and 1.10, respectively.

Table 3.7 Effects of Factors on Swelling Ratio.

Run #	M (Da)	P (% w/v)	N (% w/v)	Swelling Ratio
1	3.4 k	10	2	12.79
2	8 k	10	4	19.05
3	8 k	15	2	17.31
4	3.4 k	15	4	9.95

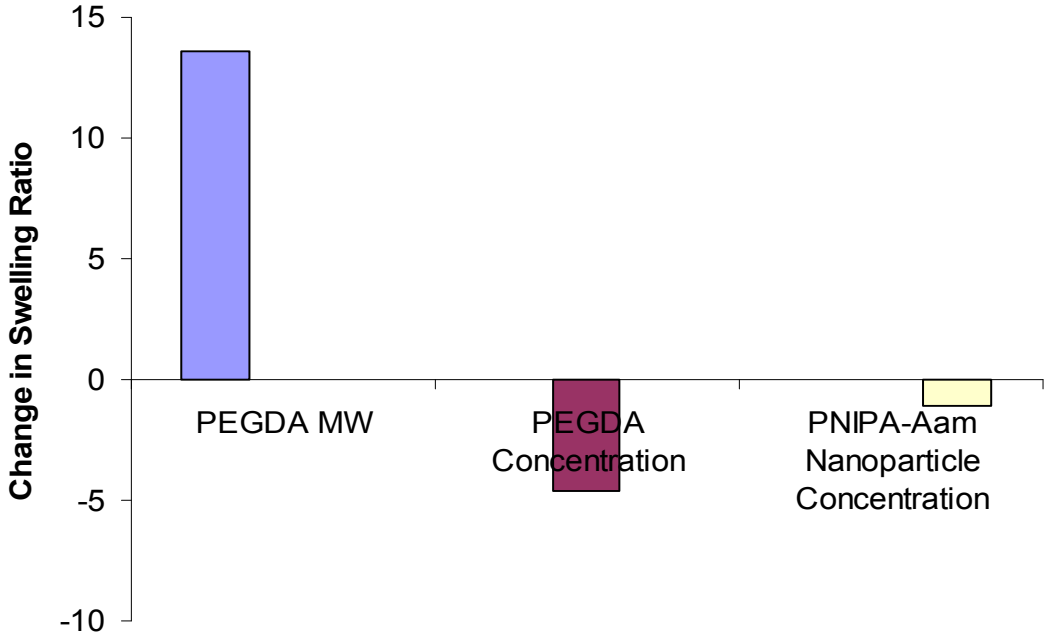

Figure 3.19 Effect of the factors on the hydrogel swelling ratio.

Figures 3.20 (a) and (b) show the variations in swelling ratio as a function of PNIPA-AAm nanoparticle concentration and PEGDA concentration at low and high levels of the most significant factor, PEGDA MW.

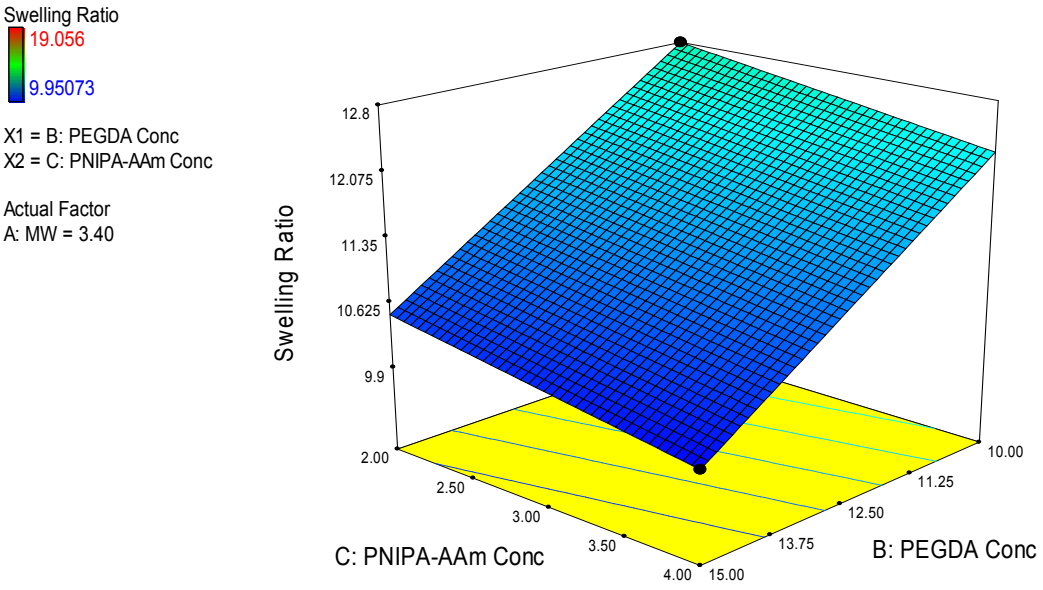

(a)

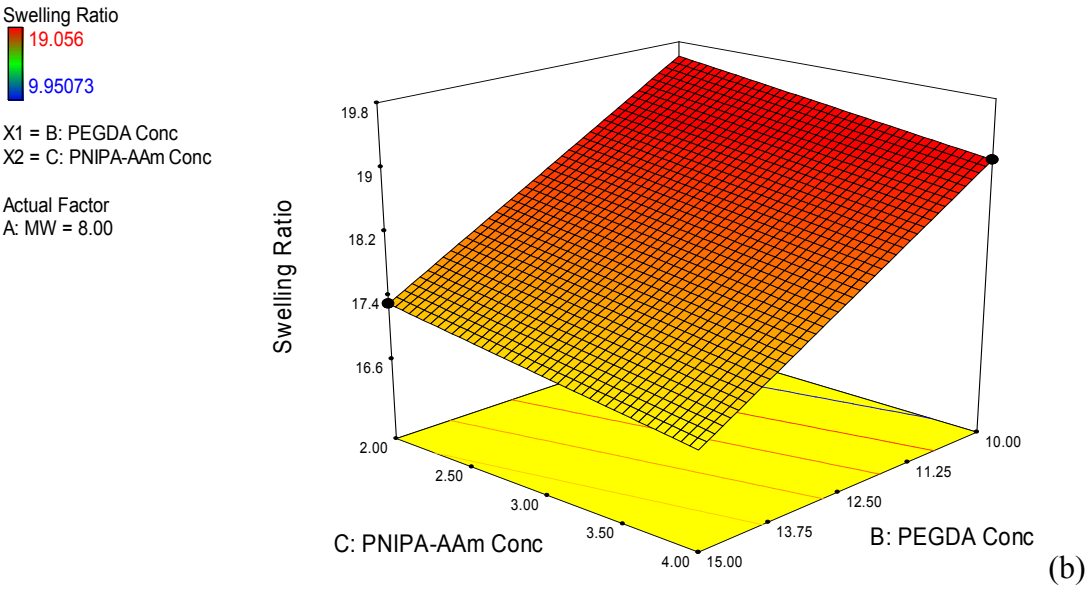

(b)

Figure 3.20 Variation in swelling ratio with (a) 3.4 kDa and (b) 8 kDa MW PEGDA.

3.4 Discussion

The characteristics of photopolymerizable hydrogel systems, such as gelation time, drug release and swelling ratio are affected by its components, namely, the PEGDA (cross-linker) MW and concentration as well as the PNIPA-AAm nanoparticle concentration. In addition, for a thermoresponsive hydrogel system, it was important to evaluate how these factors affected the thermoresponsive behavior of the system. Thus, a factorial design was prepared to evaluate the effects of the factors on the hydrogel characteristics. Experiments were performed based on this factorial design and the results were subjected to factorial analysis which helped in elucidating the factorial influences on the hydrogel characteristics.

To evaluate the effects of the factors on gelation time, hydrogels from different runs of the factorial design were formed and their gelation times were measured (Table 3.4). It was found that as factors were changed from low to high levels, all factors resulted in a decrease in gelation time (Figure 3.1). However, for reducing gelation time, PEGDA concentration was the most important factor and results showed gelation time was inversely proportional to the PEGDA concentration. Previously, results by Ghosh *et al.* have shown that increasing gelation times (from 5 to 19 minutes) are observed as PEGDA concentration is reduced from 9% to 3% (w/v) in thiol-functionalized hyaluronan PEGDA hydrogels.[56] These lower gelation times observed in high 9% w/v) PEGDA concentration hydrogels are due to the increased number of cross-links formed, as a result of higher PEGDA concentration.[56] Therefore, it is possible that more number of binding sites are present and result in a reduced time

required to form the 3-dimensional gel network as a result of higher PEGDA concentrations.

The drug release from the composite systems was divided into two parts, namely, drug release profiles and thermoresponsiveness. From figure 3.3, different amounts of drug were released by composite systems from different runs during the same time period, making it important to analyze the factorial influence. Similarly, from figure 3.5, it is seen that the difference in drug release rates between 25^{o}C and 40^{o}C are not same for the 4 runs, i.e. each run shows a varying degree of thermoresponsive behavior, making it important to understand how different factorial combinations affected the thermoresponsive behavior of the composite systems.

The factorial analysis of drug release rates over 48 hours showed that PEGDA concentration had the most significant effect on the drug release at 25^{o}C (Figure 3.6). It is reported that the higher PEGDA concentration presents greater number of cross-links.[56] These increased number of cross-links might affect the network structure by forming a denser and close-knit network, thereby hindering the drug release. Additionally, increasing the PEGDA MW weight to 8 kDa resulted in an increased drug release rate (Figure 3.6). The higher cross-linker MW may produce a network in which the cross-links are formed farther apart from each other (due to longer chain length) when compared to the lower MW network, thereby resulting in a more "porous" network. The more porous network might allow easier diffusion of the released drug and hence a higher release rate. It has also been previously reported that an increase in molecular weight might increase the pore sizes of the PEGDA hydrogel networks.[35]

Finally, since the LCST of the PNIPA-AAm nanoparticles is higher than 25^{o}C, the drug release rate is affected by the nanoparticle concentration to a lesser extent at 25^{o}C (below LCST) when compared to PEGDA MW and concentration.

In contrast to drug release at 25^{o}C, the factorial analysis of the drug release profile at 40^{o}C revealed that PNIPA-AAm nanoparticle concentration was the most significant factor (Figure 3.8). In contrast, both PEGDA MW and concentration did not have a significant effect on the release rate. At 40^{o}C, i.e. LCST of PNIPA-AAm, the structure of the PNIPA-AAm nanoparticles undergoes a sharp phase transition from coil to globule conformation and exhibits hydrophobic behavior.[34] Thus, most of the hydrophilic drug is expelled out of the PNIPA-AAm nanoparticles as the nanoparticles collapse above the LCST. Therefore, the drug release profiles at 40^{o}C are completely governed by the phase transition of the PNIPA-AAm nanoparticles. As the PNIPA-AAm nanoparticle concentration was increased (2% to 4% w/v), a higher drug release was induced showing PNIPA-AAm nanoparticle concentration was the most significant effect on the drug release at 40^{o}C.

Since our drug release profiles are biphasic for all 4 runs (Figure 3.3), it is important to consider the factorial influence on drug release during the two separate phases (burst and plateau). Additionally, since the thermoresponsiveness of the 4 runs has already been established, only the drug release at 40^{o}C has been further investigated. The release profiles exhibit an initial burst release (up to 8 hours) where most of the protein is released. Following the burst phase, the profile shows a plateau region (8 to 48 hours) exhibiting a slow sustained drug release. During the first 8 hours,

the factorial analysis showed that PNIPA-AAm nanoparticle affected the release rate most significantly (Figure 3.11). It is possible that PNIPA-AAm phase transition is the major factor in deciding the drug release rate. Most of the drug will be released when the PNIPA-AAm nanoparticles' structures collapse and expel the drug. Contrary to the initial burst period, the factorial analysis showed that, PNIPA-AAm nanoparticle concentration was not the deciding factor for drug release rate and only had a small positive effect during the plateau region (Figure 3.14). On the other hand, PEGDA MW was able to increase the drug release rates most significantly during the plateau region of the drug release profile at 40^{o}C. Since drug release out of the composite system occurs through diffusion, the "porosity" of the high MW PEGDA allows better diffusion of the drug entrapped in the network and thereby presents the higher drug release rate during the later period.

To evaluate the dependence of thermoresponsiveness on the 3 factors, we calculated the difference between the drug release rates at both temperatures, i.e. 25^{o}C and 40^{o}C for the first 8 hours (Figure 3.24). Since the thermoresponsive behavior was evident in the first 8 hours, only the drug release rates from this period were considered. The factorial analysis determined that PNIPA-AAm nanoparticle concentration was the most significant factor in affecting the thermoresponsiveness. As PNIPA-AAm nanoparticles are the only thermoresponsive components of the system, it is obvious that they would have the greatest effect on the thermoresponsiveness. However, it is interesting to note that PEGDA MW has a negative effect on thermoresponsiveness. Similarly, PEGDA concentration has a positive effect on the thermoresponsiveness. It

is possible that these 2 factors affect thermoresponsiveness by affecting the diffusion of the drug already expelled by nanoparticles but entrapped in the hydrogel network.

Finally, the factorial analysis on the swelling ratio data showed that PEGDA MW had the highest effect on the swelling ability of hydrogels, with more swelling observed as the MW increased (Figure 3.19). DiRamio *et al.* have also shown previously that for their PEG methacrylate/dimethacrylate hydrogels, the swelling ratios increased as the MW of the cross-linker increased.[57] Evaluating the hydrogel swelling ratios was important as it further corroborated the theory that the lower MW cross-linker would have shorter chains than high MW cross-linker, and thus form a tighter and more compact network due to the closer cross-links. Therefore, as low MW cross-linker will not allow hydrogel to swell sufficiently (compared to high MW), diffusion of the water into and drug out of the hydrogel is limited. This explains how increasing the PEGDA MW had a positive effect on the hydrogel drug release studies.

3.5 Conclusion

The factorial analysis was performed to evaluate the effects of 3 factors (PEGDA MW and concentration, and PNIPA-AAm nanoparticle concentration) on gelation time, drug release, thermoresponsiveness and swelling ratio of the hydrogels. PEGDA concentration was found to have the most significant effect on lowering gelation time. For drug release, at 40^{o}C, PNIPA-AAm nanoparticle concentration was shown to affect drug release most significantly during the initial burst region while PEGDA MW governed release in the plateau region. PNIPA-AAm nanoparticle

concentration was the major factor controlling degree of thermoresponsiveness of the hydrogel systems. Further, for swelling ratio, PEGDA MW was found to be the most important factor. Therefore, on the basis of the factorial analysis study, a system could be chosen with appropriate levels of these 3 factors to tailor the system and obtain desired system characteristics.

CHAPTER 4

CONCLUSION

The overall goal of our project was to develop the 3D photopolymerizable thermoresponsive composite nanoparticle hydrogels as controlled drug delivery systems for wound healing and restenosis applications. The specific aims were to evaluate the cytotoxicity of the composite system and perform factorial analysis to gain a better understanding of factors governing the system characteristics. Cytotoxicity studies on HASMCs and NIH/3T3 fibroblasts revealed that the photoinitiator and free radicals released during photopolymerization were the most cytotoxic factors. Further, the cytotoxicity of the photoinitiator at same concentrations was found to be different for both cell types. Additionally, although use of ascorbic acid improved cell survival, gelation times were increased which may potentially cause additional cell toxicity due to the prolonged exposure times.

In addition to the cytotoxicity evaluation, the factorial analysis was performed to evaluate the effects of 3 factors (PEGDA MW, PEGDA concentration, and PNIPA-AAm nanoparticle concentration) on gelation time, drug release, thermoresponsiveness and swelling ratio of the composite systems. Based on the factorial analysis study, the influence of each individual factor on the different system characteristics was delineated. The most significant factor affecting each composite system output was also identified. Using this information, future composite systems can be accurately

designed to have specific drug release profiles, thermoresponsive behavior, or structural properties while maintaining the system's biocompatibility.

CHAPTER 5

LIMITATIONS AND FUTURE WORK

The cytotoxic evaluation and factorial analysis undertaken in this project were initial steps towards developing the 3D photopolymerizable thermoresponsive composite hydrogel nanoparticle system for use in wound healing and prevention of restenosis. Some limitations observed in our system are noted below:

- For restenosis application, delivery of the precursor solution and subsequent UV irradiation may be difficult. This limitation might be overcome by using newer technologies such as microporous balloon catheter for delivery and UV optical fibers for irradiation.
- Gelation times need to be minimized to use this system in prevention of restenosis. This limitation can be overcome by finding a trade-off between photoinitiator concentration, PEGDA concentration and the biocompatibility of the system.
- Since drug loading onto PNIPA-AAm nanoparticles is done below its LCST, the drugs chosen must be hydrophilic in nature.

Some suggestions for future work include:

- Rheological experiments must be conducted to evaluate the strength of the composite hydrogels.

- Shear stress studies will need to be conducted to test the system's ability to adhere to the arterial wall after implantation.
- PNIPA-AAm nanoparticles may be modified to prolong the drug release from the composite hydrogels. B-cyclodextrin has been used successfully for this purpose by other groups by forming inclusion complexes with the drug.[58]
- Modifications to obtain a faster response of PNIPA-AAm to temperature changes should be investigated. This will help in improved control of delivering drugs in an on-off fashion.
- Investigation of other anti-oxidants in reducing the cytotoxicity while maintaining gelation times should be performed.

REFERENCES

1. http://www.angioplasty.org/nv/angio101.html.
2. http://www.managedcaremag.com/archives/0307/0307.biotech.html.
3. Rivard A, Andrâes V. Vascular smooth muscle cell proliferation in the pathogenesis of atherosclerotic cardiovascular diseases. Histology and histopathology 2000;15(2):557-71.
4. Indolfi C, Coppola C, Torella D, Arcucci O, Chiariello M. Gene therapy for restenosis after balloon angioplasty and stenting. Cardiology in review 1999;7(6):324-31.
5. Ip JH, Fuster V, Badimon L, Badimon J, Taubman MB, Chesebro JH. Syndromes of accelerated atherosclerosis: role of vascular injury and smooth muscle cell proliferation. Journal of the American College of Cardiology 1990;15(7):1667-87.
6. Kavanagh CA, Rochev YA, Gallagher WM, Dawson KA, Keenan AK. Local drug delivery in restenosis injury: thermoresponsive co-polymers as potential drug delivery systems. Pharmacol Ther 2004;102(1):1-15.
7. Luscher TF, Steffel J, Eberli FR, Joner M, Nakazawa G, Tanner FC, Virmani R. Drug-eluting stent and coronary thrombosis: biological mechanisms and clinical implications. Circulation 2007;115(8):1051-8.

8. Leon MB. Late thrombosis a concern with drug-eluting stents. J Interv Cardiol 2007;20(1):26-9.

9. Wenaweser P, Dorffler-Melly J, Imboden K, Windecker S, Togni M, Meier B, Haeberli A, Hess OM. Stent thrombosis is associated with an impaired response to antiplatelet therapy. J Am Coll Cardiol 2005;45(11):1748-52.

10. Braddock M, Campbell CJ, Zuder D. Current therapies for wound healing: electrical stimulation, biological therapeutics, and the potential for gene therapy. Int J Dermatol 1999;38(11):808-17.

11. Ishihara M, Nakanishi K, Ono K, Sato M, Kikuchi M, Saito Y, Yura H, Matsui T, Hattori H, Uenoyama M and others. Photocrosslinkable chitosan as a dressing for wound occlusion and accelerator in healing process. Biomaterials 2002;23(3):833-40.

12. Turner TD. Hospital usage of absorbent dressings. Pharma J 1979;222:421-426.

13. Eaglstein WH. Moist wound healing with occlusive dressings: a clinical focus. Dermatol Surg 2001;27(2):175-81.

14. Keast DH, Orsted H. The basic principles of wound care. Ostomy Wound Manage 1998;44(8):24-8, 30-1.

15. An Y, Hubbell JA. Intraarterial protein delivery via intimally adherent bilayer hydrogels. J Control Release 2000(64):205-15.

16. Chowdhury SM, Hubbell JA. Adhesion prevention with ancrod released via a tissue-adherent hydrogel. J Surg Res 1996;61(1):58-64.

17. Lu S, Anseth KS. Photopolymerization of multilaminated poly(HEMA) hydrogels for controlled release. J Control Release 1999;57(3):291-300.

18. Peppas NA, Keys KB, Torres-Lugo M, Lowman AM. Poly(ethylene glycol)-containing hydrogels in drug delivery. J Control Release 1999;62(1-2):81-7.

19. Scott RA, Peppas NA. Highly crosslinked, PEG-containing copolymers for sustained solute delivery. Biomaterials 1999;20(15):1371-80.

20. Cruise GM, Hegre OD, Lamberti FV, Hager SR, Hill R, Scharp DS, Hubbell JA. In vitro and in vivo performance of porcine islets encapsulated in interfacially photopolymerized poly(ethylene glycol) diacrylate membranes. Cell Transplant 1999;8(3):293-306.

21. Cruise GM, Hegre OD, Scharp DS, Hubbell JA. A sensitivity study of the key parameters in the interfacial photopolymerization of poly(ethylene glycol) diacrylate upon porcine islets. Biotechnol Bioeng 1998;57(6):655-65.

22. Hill RS, Cruise GM, Hager SR, Lamberti FV, Yu X, Garufis CL, Yu Y, Mundwiler KE, Cole JF, Hubbell JA and others. Immunoisolation of adult porcine islets for the treatment of diabetes mellitus. The use of photopolymerizable polyethylene glycol in the conformal coating of mass-isolated porcine islets. Ann N Y Acad Sci 1997;831:332-43.

23. Elisseeff J, McIntosh W, Anseth K, Riley S, Ragan P, Langer R. Photoencapsulation of chondrocytes in poly(ethylene oxide)-based semi-interpenetrating networks. J Biomed Mater Res 2000;51(2):164-71.

24. Elisseeff J, Anseth K, Sims D, McIntosh W, Randolph M, Langer R. Transdermal photopolymerization for minimally invasive implantation. Proc Natl Acad Sci U S A 1999;96(6):3104-7.

25. Elisseeff J, Anseth K, Sims D, McIntosh W, Randolph M, Yaremchuk M, Langer R. Transdermal photopolymerization of poly(ethylene oxide)-based injectable hydrogels for tissue-engineered cartilage. Plast Reconstr Surg 1999;104(4):1014-22.

26. Sawhney AS, Pathak CP, Hubbell JA. Interfacial photopolymerization of poly(ethylene glycol)-based hydrogels upon alginate-poly(l-lysine) microcapsules for enhanced biocompatibility. Biomaterials 1993;14(13):1008-16.

27. Cruise GM, Scharp DS, Hubbell JA. Characterization of permeability and network structure of interfacially photopolymerized poly(ethylene glycol) diacrylate hydrogels. Biomaterials 1998;19(14):1287-94.

28. Pathak CP, Sawhney AS. Rapid photopolymerization of immunoprotective gels in contact with cells and tissue. J Am Chem Soc 1992(114):8311-2.

29. Bryant SJ, Nuttelman CR, Anseth KS. Cytocompatibility of UV and visible light photoinitiating systems on cultured NIH/3T3 fibroblasts in vitro. J Biomater Sci Polym Ed 2000;11(5):439-57.

30. Nguyen KT, West JL. Photopolymerizable hydrogels for tissue engineering applications. Biomaterials 2002;23(22):4307-14.

31. Williams CG, Malik AN, Kim TK, Manson PN, Elisseeff JH. Variable cytocompatibility of six cell lines with photoinitiators used for polymerizing hydrogels and cell encapsulation. Biomaterials 2005;26(11):1211-8.

32. Quick DJ, Anseth KS. DNA delivery from photocrosslinked PEG hydrogels: encapsulation efficiency, release profiles, and DNA quality. J Control Release 2004;96(2):341-51.

33. Quick DJ, Macdonald KK, Anseth KS. Delivering DNA from photocrosslinked, surface eroding polyanhydrides. J Control Release 2004;97(2):333-43.

34. Ramanan RM, Chellamuthu P, Tang L, Nguyen KT. Development of a temperature-sensitive composite hydrogel for drug delivery applications. Biotechnol Prog 2006;22(1):118-25.

35. Bhadra D, Bhadra S, Jain P, Jain NK. Pegnology: a review of PEG-ylated systems. Pharmazie 2002;57(1):5-29.

36. Piskin E, Dincer S, Turk M. Gene delivery: intelligent but just at the beginning. J Biomater Sci Polym Ed 2004;15(9):1181-202.

37. Hirose M, Yamato M, Kwon OH, Harimoto M, Kushida A, Shimizu T, Kikuchi A, Okano T. Temperature-Responsive surface for novel co-culture systems of hepatocytes with endothelial cells: 2-D patterned and double layered co-cultures. Yonsei Med J 2000;41(6):803-13.

38. Galaev I, Mattiasson B. Thermoreactive water-soluble polymers, nonionic surfactants, and hydrogels as reagents in biotechnology. Enzyme Microb Technol 1993;15(5):354-66.

39. Vernon B, Kim SW, Bae YH. Thermoreversible copolymer gels for extracellular matrix. J Biomed Mater Res 2000;51(1):69-79.

40. Chung JE, Yokoyama M, Yamato M, Aoyagi T, Sakurai Y, Okano T. Thermo-responsive drug delivery from polymeric micelles constructed using block copolymers of poly(N-isopropylacrylamide) and poly(butylmethacrylate). J Control Release 1999;62(1-2):115-27.

41. Jeong B, Bae YH, Lee DS, Kim SW. Biodegradable block copolymers as injectable drug-delivery systems. Nature 1997;388(6645):860-2.

42. Kikuchi A, Okano T. Pulsatile drug release control using hydrogels. Adv Drug Deliv Rev 2002;54(1):53-77.

43. Neradovic D, Soga O, Van Nostrum CF, Hennink WE. The effect of the processing and formulation parameters on the size of nanoparticles based on block copolymers of poly(ethylene glycol) and poly(N-isopropylacrylamide) with and without hydrolytically sensitive groups. Biomaterials 2004;25(12):2409-18.

44. Hill-West JL, Chowdhury SM, Slepian MJ, Hubbell JA. Inhibition of thrombosis and intimal thickening by in situ photopolymerization of thin hydrogel barriers. Proc Natl Acad Sci U S A 1994;91(13):5967-71.

45. Atsumi T, Murata J, Kamiyanagi I, Fujisawa S, Ueha T. Cytotoxicity of photosensitizers camphorquinone and 9-fluorenone with visible light irradiation on a human submandibular-duct cell line in vitro. Arch Oral Biol 1998;43(1):73-81.

46. Wu JY, Liu SQ, Heng PW, Yang YY. Evaluating proteins release from, and their interactions with, thermosensitive poly (N-isopropylacrylamide) hydrogels. J Control Release 2005;102(2):361-72.

47. Gao J, Hu Z. Optical properties of *N*-isopropylacrylamide microgel spheres in water. Langmuir 2002(18):1360-67.

48. Hanks CT, Strawn SE, Wataha JC, Craig RG. Cytotoxic effects of resin components on cultured mammalian fibroblasts. J Dent Res 1991;70(11):1450-5.

49. Manevich Y, Sweitzer T, Pak JH, Feinstein SI, Muzykantov V, Fisher AB. 1-Cys peroxiredoxin overexpression protects cells against phospholipid peroxidation-mediated membrane damage. Proc Natl Acad Sci U S A 2002;99(18):11599-604.

50. Naji L, Carrillo-Vico A, Guerrero JM, Calvo JR. Expression of membrane and nuclear melatonin receptors in mouse peripheral organs. Life Sci 2004;74(18):2227-36.

51. Rodriguez C, Mayo JC, Sainz RM, Antolin I, Herrera F, Martin V, Reiter RJ. Regulation of antioxidant enzymes: a significant role for melatonin. J Pineal Res 2004;36(1):1-9.

52. Bonorden WR, Pariza MW. Antioxidant nutrients and protection from free radicals. New York: Raven Press; 1994.

53. Fang YZ, Yang S, Wu G. Free radicals, antioxidants, and nutrition. Nutrition 2002;18(10):872-9.

54. DeLong SA, Moon JJ, West JL. Covalently immobilized gradients of bFGF on hydrogel scaffolds for directed cell migration. Biomaterials 2005;26(16):3227-34.

55. Nuttelman CR, Tripodi MC, Anseth KS. In vitro osteogenic differentiation of human mesenchymal stem cells photoencapsulated in PEG hydrogels. J Biomed Mater Res A 2004;68(4):773-82.

56. Ghosh K, Shu XZ, Mou R, Lombardi J, Prestwich GD, Rafailovich MH, Clark RA. Rheological characterization of in situ cross-linkable hyaluronan hydrogels. Biomacromolecules 2005;6(5):2857-65.

57. Diramio JA, Kisaalita WS, Majetich GF, Shimkus JM. Poly(ethylene glycol) methacrylate/dimethacrylate hydrogels for controlled release of hydrophobic drugs. Biotechnol Prog 2005;21(4):1281-8.

58. Zhang JT, Huang SW, Liu J, Zhuo RX. Temperature sensitive poly[N-isopropylacrylamide-co-(acryloyl beta-cyclodextrin)] for improved drug release. Macromol Biosci 2005;5(3):192-6.

BIOGRAPHICAL INFORMATION

Abhimanyu Sabnis was born in Mumbai, India in April 1983. He graduated with a Bachelor of Engineering degree in Biomedical Engineering from the Visveswaraya Technological University, India in June 2005. After enrolling in the Biomedical Engineering program at the University of Texas at Arlington in August 2005, he began conducting research under the guidance of Dr. Kytai Nguyen. His research interests include drug delivery, biomaterials and tissue engineering. Upon completion of the Master of Science degree in Biomedical Engineering at UT, Arlington, he intends to gain industrial experience before pursuing a Ph.D. degree in the same field.